Chapter 4
Theory of Tethered Aerial Vehicles

4.1 Related Works and Problem Statement

Driven by the relevance of this topic, several control and estimation schemes have been presented in the robotic literature. For the case in which the aerial vehicle is an helicopter, the authors of [1] presented a method to land it on the deck of a ship in rough sea using a cable. The controller is based on a time-scale separation technique between the rotational and translational dynamics. In the context of [2], the authors of [3] presented a control scheme based on a PID scheme together with partial model inversion, to stabilize the flight to a constant vertical elevation with the goal of both improving hovering in windy conditions and land on a mobile platform. Notice that a force sensor (load cell) is used to measure the tension along the cable and to compensate its effect on the vehicle. The latter work has been then extended to a tether aerial vehicle together with a winch, in order to perform the landing of a small unmanned helicopter, without the use of GPS sensors but relying on simpler magnetic encoders [4]. Furthermore, in [5] the authors proposed a square-root unscented Kalman filter for the estimation of the attitude and the relative position of the vehicle with respect to the ground anchoring point.

For the case of cable-tethered underactuated multi-rotor system moving on a restricted 2D vertical plane, [6] presents a controller that, under a quasi-static assumption, stabilizes the elevation (angle) of the cable to a constant value using only inertial onboard sensors. In particular, the controller is based on the separation of the translational and rotational dynamics, and on a partial inversion of the elevation dynamics where they fix the total thrust to a value sufficiently high to preserve the tautness of the cable. The state estimator is instead based on a UKF. The authors of [7, 8] also present a controller to stabilize the elevation of a tethered multi-rotor to a constant value while also ensuring the positivity of the cable tension. The controller is based on the combination of a hierarchical cascade approach to stabilize the system and a reference governor to ensure a positive internal tension.

M. Tognon and A. Franchi, *Theory and Applications for Control of Aerial Robots in Physical Interaction Through Tethers*, Springer Tracts in Advanced Robotics 140,
https://doi.org/10.1007/978-3-030-48659-4_4

The presented approaches provide a good basis for observation and control of such systems. However, to improve those methods, overcoming some of their drawbacks, and to extends the results to a more general system, some problems have to to be addressed:

(i) study a more *generic system* in order to enlarge the validity of the results. In particular one could think about three extensions of the classical tethered aerial vehicle: *(i)* Develop a method that can cope with *any kind of link* (i.e., a cable, a strut or a bar), differently from the state-of-the-art methods, which have been designed only for cable links. Indeed the use of rigid link can be beneficial for, e.g., sustain part of the platform weight, or allow a full-bilateral physical interaction with a ground object. *(ii)* Furthermore, instead of considering a static anchoring point, one could consider a *generic platform* moving in the 3D environment, without particular constraints. This allows to consider a very wide class of possible vehicles. *(iii)* Finally one could consider a *link actuator* in order to be able to also change the length of the link, thus controlling the full 3D position of the aerial vehicle with respect to the moving platform.

(ii) *track a time varying trajectory*. While the methods in the literature are based on a quasi-static assumption aiming to a stabilization problem, in many practical cases it is important to track a time-varying trajectory to, e.g., let the aerial robot track a moving target.

(iii) *track a desired link force profile*. In many cases it is important to precisely regulate the force link to any desired value, possibly including negative link force (pushing) if the link is a bar. For example, if the link is a cable, one may want to keep it always taut while at the same time avoiding peaks on the tension that can damage the cable or its attaching mechanisms. If the link is a bar, then one may want to push against it with an appropriate force to perform physical interaction with the environment. However, the methods in the literature are able, in the best case [7], to keep the force link positive, but not at a prescribed value, possibly time-varying.

(iv) *observe the state* from a minimal set of sensors in any dynamic condition. Instead, in the state-of-the-art this is done at best in a quasi-static assumption or with a linearized method [4, 6].

Table 4.1 shows the features of the methods proposed in the state of the art and of the ones proposed in this book.

In order to achieve the previous objectives, a thoroughly analysis of the system from a theoretical point of view is needed. This is why, one of the goal of this book is to provide a fundamental study of the tethered aerial vehicle system, in order to have a clear understanding of its dynamics and the corresponding properties related to control, planning and estimation. Our formal analysis is focused on three main objectives along the axes of control, planning and localization:

(1) Find the output for which it is possible to compute analytically and offline the state of the system while exactly tracking the desired output trajectory, and the nominal inputs required to do so. This option is very useful for control, to compute

Table 4.1 Features of the methods proposed by the state of the art and of the ones proposed in this book

	[3–5]	[6]	[7, 8]	This book
Stabilization of the position	✓	✓	✓	✓
Taut cable ensured			✓	✓
Control of tension and compression				✓
Independent tracking of position and internal force				✓
Independent tracking of position and partial attitude				✓
2D state estimation with IMU only		✓		✓
3D state estimation with IMU plus encoders	✓			✓
Global state estimation				✓

the feed-forward terms, and in a possible pre-planning strategy. To achieve this objective we investigate which are the *flat outputs* and we explicit the algebraic relations that demonstrate the *differential flatness* of the system (see Sect. 4.4).

(2) For each of the found set of flat outputs, given any desired sufficiently smooth trajectory, we aim at designing a control strategy to obtain the exact trajectory tracking (see Sect. 4.6). The control method will be based on the static or dynamic (if needed) *feedback linearization* method presented in Sect. 2.3.

(3) Provide the mathematical tools to implement the control strategy in a real world using a minimal set of typically available on-board sensors. For this goal, we propose a minimal standard sensory equipment and we show how to design an almost global nonlinear observer in order to estimate the state from the available measurements only. This enables the possibility to close the control loop with standard and minimal measurements (see Sects. 4.7 and 4.8).

Based on these results, practical problems coming from applicative scenarios can be solved more easily. An example can be found in Chap. 6 where we exploited the theoretical results to solve the practical but challenging problem of landing and takeoff on/from highly sloped surfaces.

4.2 Contribution

This part of the book provides a thorough analysis of a generic tethered system in which we formally study the dynamics of the system and its intrinsic properties, along the three major axes of control, planning and estimation.

Firstly we consider a much more generic tethered system that extends the previously considered system by four major points. Indeed, we analyze a system firstly composed by an *unidirectional-thrust aerial vehicle flying in the 3D space* (not only in a 2D plane as some of the related publications). The vehicle is attached by a *generic link* to an *independently moving platform*. Differently from the state of the art where only the cable case is considered, here the generic link can be either a cable, a strut or a bar. In this way we can consider links that can be:

(i) only stretched, like cables, that allow only positive internal forces called tensions;
(ii) only compressed, like strut, that allow only negative internal forces called compression;
(iii) both compressed and stretched, like bars, that allow both positive and negative internal forces.

At the other end, the link is attached to a platform that can independently move in the 3D space. Differently from the related literature where the link is anchored to a fixed point, in this book we consider a much generic case in which the link could be attached to a car, a sheep, another aircraft, or even to a human operator.

Finally, for the sake of generality, we consider that a *link actuator* is capable of changing the length of the link applying a certain controllable force. This device can be a winch in the case of a cable-link, or an actuated telescopic mechanism in the case of a bar-link. The modeling of this generic system is provided in Sect. 4.3.

We started our analysis with the investigation of the *differential flatness* property, looking for the sets of flat outputs (if more then one). We proved that the system is differentially flat with respect to two outputs $\mathbf{y}^a$ and $\mathbf{y}^b$.

(a) $\mathbf{y}^a$ is a *force-related output*. It contains the position of the vehicle with respect to the moving platform (expressed in spherical coordinates), the internal force along the link, and the rotation of the vehicle along the thrust axis (see Sect. 4.6.1). This shows that the position and the internal force along the link can be controlled independently. Notice the parallel with hybrid motion/force control of ground manipulators in the presence of kinematic constraints [9].
(b) $\mathbf{y}^b$ is an *attitude-related output*. It contains the position of the vehicle with respect to the moving platform, a particular angle related to the attitude of the vehicle with respect to the one of the link, and the rotation of the vehicle along the thrust axis (see Sect. 4.6.2). This shows that the position and this particularly defined angle can be controlled independently.

These are in turn *flat outputs* for the system. This property fulfills the planning related objective, and allows to know in advance the nominal state and inputs while exactly tracking a desired output trajectory.

For the two sets of flat outputs we then designed a hierarchical controller based on the separation between the rotational and translational dynamics controllers (see Sect. 4.5). We designed this controller with the aim of stabilizing the flat outputs to a desired value, keeping it simple to implement also for commercially available aerial vehicle for which one can control only the attitude or, at best, the angular velocity. However, after the experimental validation, we noticed that this controller cannot provide good tracking performance when the desired trajectory requires high velocities and acceleration. In particular, this is due the separation assumption between translational and rotation dynamics.

To fulfill the tracking control objective, we then studied the feedback linearizability of the system with respect to $\mathbf{y}^a$ and $\mathbf{y}^b$. Once we proved that $\mathbf{y}^a$ and $\mathbf{y}^b$ are flat output for the considered system, we know that they are also feedback linearizing outputs. Indeed, it exists a feedback control law that linearizes the relation input-output. Then a controller based on the Dynamic Feedback Linearization (DFL) method has been conceived for the tracking of the two sets of outputs, highlighting the related singularities, extended relative degree and the required dynamic extension. Notice that the works in the state of the art considered only the problem of regulating the position of the vehicle (mostly in the 2D case), at most ensuring the positivity of the internal force. On the other hand, in this work we derived a control for the precise tracking of any time-varying desired position and internal force trajectories. Furthermore, we also designed a controller for the precise tracking of a different and never considered output: position plus attitude-related variable.

Finally, for the estimation objective, we showed that if the motion of the moving platform is known, then the state of the system can be estimated using only the onboard IMU and three encoders placed at the other end of the link in order to measure its attitude and length. We then found some nonlinear measurements transformations that allowed us to employ the nonlinear High Gain Observer (presented in Sect. 2.4) to get an estimation of the state and close the control loop preserving the stability of the overall system (see Sect. 4.7).

This theoretical and fundamental results have been extensively validated either experimentally or through numerical simulations. The first implemented hierarchical controller has been validated experimentally and employed for the execution of landing and takeoff on/from a sloped surface as well. The corresponding results are presented in Chap. 5.

The rest of the theoretical results has been instead validated by a deep simulation campaign. We also analyzed the limits of the methods under non ideal conditions such as noisy measurements, parameter uncertainties, etc. Only the dynamic feedback linearizing controller for the output $\mathbf{y}^b$ has not been validated yet. Indeed, we proved the feedback linearizability of the system with respect to $\mathbf{y}^b$ only very recently, without having the possibility to conduct a validating campaign. This will be done in the near future. For the same reason, notice that this results has not been published neither. On the other hand, all the other results related to the control of $\mathbf{y}^a$ and the state estimation problems has been published in [10]. The proof of the differential flatness with respect to $\mathbf{y}^b$ and the design of a hierarchical control to track a desired trajectory of $\mathbf{y}^b$ have been partially presented in [11].

All the previous mentioned results are obviously still valid if there is not a link actuator and the link length is fixed, if the platform is still, and even if the system motion is constrained on a 2D vertical plane. On the other hand, in this particular constrained case, we proved a very interesting result. We showed that only the on-board IMU is needed to retrieve the estimation of the state. Also in this case, we found some non linear measurements and state transformations that bring the system in a canonical form for which the High Gain Observer can be applied. These results have been published in [12, 13].

We also considered another interesting particular case, i.e., when the link actuator is not active but *passive*. In this case the force produced by the link actuator is constant and cannot be controlled. One could made this mechanism with simple springs, like in a retractable leash. This solution simplifies the complexity of the system and reduces the weight as well, thus its could be preferable in some cases, e.g., to make the system easily portable by a human operator. The only controllable actuation is then given by the orientable thrust generated by the underactuated aerial vehicle. Having one controllable actuator less, it appears that the internal force along the link is not controllable anymore, and the attitude angle neither. We proved that only the output $\mathbf{y}^c$, containing the position of the vehicle and its rotation about the thrust axis, is a differentially flat/dynamic feedback linearizable output (see Sects. 4.4.3 and 4.6.3). These results have been published in [14].

All the previous theoretical results constitute the base to solve practical and more application oriented problems. With a good understanding of the system in exam, one can then better exploit its properties for the accomplishment of particular tasks related to a specific applications. For example, considering the challenging problem of landing and takeoff on/from a sloped surface, e.g., in mountains for search and rescue operations, we showed that a tethered aerial vehicle could be very useful to accomplish the task in a very robust and reliable way. In Chap. 6 we theoretically and experimentally show how we exploited the theoretical results, and in particular the ones related to the controllability of $\mathbf{y}^b$, to solve the problem in a more robust way with respect to the case of a free-flying vehicle. The corresponding methods and results have been published in [11, 15]. For a more detailed introduction and state of the art relative to the problem, we refer the reader to Chap. 6.

Finally, starting from the results obtained on control and state estimation of a single tethered aerial vehicle, we performed the same type of rigorous analysis on a multi-robot system (see Chap. 7). Indeed, since the single tethered aerial vehicle is constrained to fly around the anchoring point, the working space (a simple circle in the planar case) can result very limited for some applications, such as pick and place or inspection in cluttered environments. One possible solution is given by adding a second vehicle attached to the first by a second link. In particular, we considered a system composed by two aerial vehicles laying on a vertical 2D plane, where the first one is attached to the ground and to the second one by two links, in the way of forming a chain of two elements. Considering the second robot as an end-effector, the system appears similar to a two-link planar manipulator where the aerial vehicles are the actuators. It is then clear the increased dexterity of the system. Although it might appear not feasible from a practical point of view using cable-links, actually, it could

Table 4.2 Summary of the contributions on tethered aerial vehicles

System	3D environment		Only 2D env.
One link—Active link actuator	General modeling, State estimation with IMU plus three encoders, [10], Sects. 4.3 and 4.7	Differential flatness and DFL w.r.t. $\mathbf{y}^a$, [10], Sect. 4.6.1, and Differential flatness w.r.t. $\mathbf{y}^b$ [11], DFL w.r.t. $\mathbf{y}^b$, Sect. 4.6.2	State estimation with IMU only, [12, 13], Sect. 4.8
One link—Passive link actuator		DFL and differential flatness w.r.t. $\mathbf{y}^c$, Sect. 4.6.3, [14]	
Application to the problem of landing and takeoff on/from a sloped surface	Problem formulation, condition for robust landing, comparison between free-flight and tethered solutions, Chap. 6, [11, 15]		Trajectory planning for robust maneuvers, Sect. 6.5
Multi robot extension: two linked robots in a chain configuration			Differential flatness and DFL w.r.t. $\mathbf{y}_2^a$, Sect. 7.3 [16], state estimation with IMUs plus two encoders, Sect. 7.4, [17]

be easily implemented using bar-links. Furthermore, due to the peculiarity of the system, the control of such a system is a very interesting and challenging theoretical problem. As for the single tethered case, we proved that the output composed by the elevation and the internal force of the two links is differential flat/dynamic feedback linearizable. Thus we designed a nonlinear controller based on the dynamic feedback linearization technique to achieve the independent tracking of the output entries [16]. Furthermore, we proved that the IMU on-board of the two vehicles together with two encoders, one at the base and one on the first vehicle, measuring the relative link angles, are enough to make the state observable. We then found some nonlinear measurement transformations to bring the system in the canonical form that allows to apply the High Gain Observer [17]. The validity of the method has been proven by numerical simulations. For all the related results we refer the reader to Chap. 7.

Table 4.2 schematically gathers all the contributions of this book on the field of tethered aerial vehicles. For each contribution we report the corresponding chapter or section and the papers in which the results have been published.

4.3 Modeling

In this section we provide the model of a generic tethered aerial system consisting of an *unidirectional-thrust aerial vehicle* that is tethered by a generic *link* (e.g., a cable, a rope, a chain, a bar or a strut) whose length can be changed by an *active link*

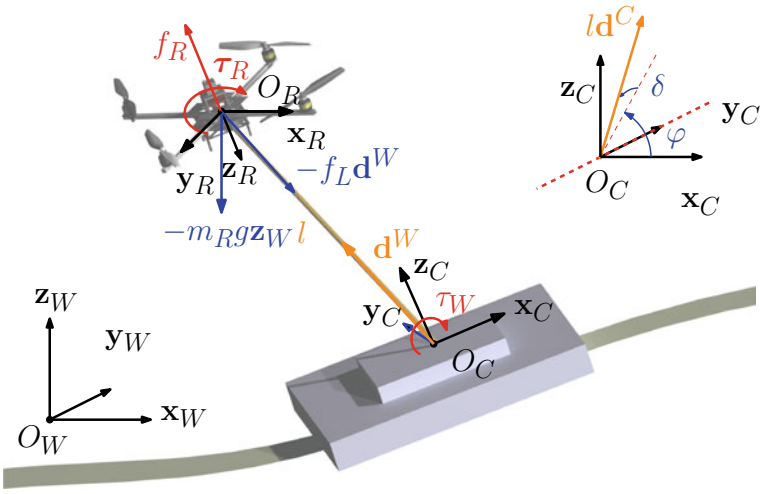

Fig. 4.1 Left: representation of the system and its main variables. Top right corner: parametrization of the unit vector $\mathbf{d}^C$. The red line shows the singularities of the parametrization, avoidable in the planning phase. © 2020 IEEE. Reprinted, with permission, from [10]

actuator. If the link is a cable-like link, then the link actuator is a winch that can roll up or unroll the link. On the other hand, if the link is a telescopic bar-like link, then the link actuator is a prismatic actuator that can extend or shorten the bar. A brief modeling of the link and of the link actuator was presented in Sects. 3.1 and 3.3.2, respectively. Although the bar-link case is not very common, it is still mechanically feasible and allows us to derive a very general model for which we can consider both positive and negative link internal forces (tensions and compressions, respectively). Doing so we expand the validity of the theoretical results. The link actuator is in turn fixed on a *moving platform* by a passive 3D spherical joint. The platform moves generically in the 3D space and can be, e.g., a ground vehicle moving on any kind of terrain, a marine vessel, or even another aerial vehicle. Figure 4.1 depicts the systems and its main definitions.

Consider a fixed *world frame*, $\mathcal{F}_W$ with axes $\{\mathbf{x}_W, \mathbf{y}_W, \mathbf{z}_W\}$ and origin O_W. In particular, $\mathbf{z}_W$ is opposite to the gravity vector. Two body frames, $\mathcal{F}_C$ and $\mathcal{F}_R$ with axes $\{\mathbf{x}_C, \mathbf{y}_C, \mathbf{z}_C\}$ and $\{\mathbf{x}_R, \mathbf{y}_R, \mathbf{z}_R\}$, and origins O_C and O_R, are rigidly attached to the platform and to the aerial vehicle, respectively. The position of O_C in $\mathcal{F}_W$ is described by the vector $\mathbf{p}_C^W = [x_C \;\; y_C \;\; z_C]^\top \in \mathbb{R}^3$. Similarly, O_R is set on the CoM of the aerial vehicle, whose position in $\mathcal{F}_W$ is described by the vector $\mathbf{p}_R^W = [x_R \;\; y_R \;\; z_R]^\top \in \mathbb{R}^3$.

Although already done in Sect. 3.2, we recall one more time the main modeling assumptions and definitions for a generic aerial vehicle. The aerial vehicle is modeled as a rigid body with mass $m_R \in \mathbb{R}_{>0}$ and positive definite diagonal inertia matrix $\mathbf{J}_R \in \mathbb{R}^{3\times3}_{>0}$ expressed in $\mathcal{F}_R$ and relative to O_R. The angular velocity of $\mathcal{F}_R$ with respect to $\mathcal{F}_W$, expressed in $\mathcal{F}_R$, is denoted by $\boldsymbol{\omega}_R \in \mathbb{R}^3$. The aerial vehicle configuration is fully described by $\mathbf{p}_R^W$ and by the rotation matrix $\mathbf{R}_R \in \mathsf{SO}(3)$, representing the position

and orientation of $\mathcal{F}_R$ w.r.t. $\mathcal{F}_W$. The aerial vehicle motion can be controlled acting on four inputs: $f_R \in \mathbb{R}$ and $\boldsymbol{\tau}_R = [\tau_{Rx} \ \tau_{Ry} \ \tau_{Rz}]^\top \in \mathbb{R}^3$, where f_R is the magnitude of the thrust force[1] $\mathbf{f}_R = -f_R \mathbf{z}_R$ applied at O_R and parallel to $\mathbf{z}_R$, and $\boldsymbol{\tau}_R$ is the control moment vector expressed in $\mathcal{F}_R$.

The moving platform configuration is described by $\mathbf{p}_C^W$ and $\mathbf{R}_C \in \mathsf{SO}(3)$, representing the rotation from $\mathcal{F}_C$ to $\mathcal{F}_W$. The angular velocity of $\mathcal{F}_C$ w.r.t. $\mathcal{F}_W$, expressed in $\mathcal{F}_C$, is denoted by $\boldsymbol{\omega}_C \in \mathbb{R}^3$. The platform is an independent sub-system whose motion *(i)* is not influenced by the aerial vehicle dynamics and *(ii)* can only be measured online. In this way, the results can be applied to a broader class of moving platforms including, e.g., human controlled vehicles.

The link connects the aerial vehicle to the moving platform. One end of the link is attached to the aerial vehicle at O_R through a passive 3D spherical joint and the other end is attached to the platform at O_C, through a second passive 3D spherical joint. Having the link directly attached to the CoM of the aerial vehicle allows to decouple the rotational dynamics to the translational one. This assumption is very common in the literature of aerial physical interaction, and is practically easy to meet. Indeed, with a wise mechanical design one can minimize the distance between the CoM and the link attaching point. As explained in Sect. 3.1, we assume negligible link mass and inertia with respect to the ones of the aerial vehicle and negligible deformations and elasticity.

The direction of the link is described by the unit vector[2] $\mathbf{d}^C \in \mathsf{S}^2$ expressed in $\mathcal{F}_C$ thus allowing to express the aerial vehicle position relative to the moving platform.[3] Nevertheless, known $\mathbf{p}_C^W$ and $\mathbf{R}_C$, one can still control $\mathbf{p}_R^W$ by inverse kinematics. The unit vector $\mathbf{d}^C$ can be parametrized with the *elevation angle*, $\varphi \in [0, 2\pi]$, and the *azimuth angle*, $\delta \in [-\frac{\pi}{2}, \frac{\pi}{2}]$, as

$$\mathbf{d}^C = \left[\cos\delta\cos\varphi \ -\sin\delta \ \cos\delta\sin\varphi\right]^\top, \tag{4.1}$$

where δ is the angle between $\mathbf{d}^C$ and the vertical plane $\{\mathbf{x}_C, \mathbf{z}_C\}$, whereas φ is the angle between the projection of $\mathbf{d}^C$ on $\{\mathbf{x}_C, \mathbf{z}_C\}$ and $\mathbf{x}_C$, see Fig. 4.1. This particular choice lets the singularity of the parametrization correspond to the points along $\mathbf{y}_C$, whereas the classical spherical parametrization has the singularity along $\mathbf{z}_C$, which corresponds to the common vertical link orientation (when, e.g., the vehicle has to fly above the moving platform).

The link length and the intensity of the internal force are denoted by $l \in \mathbb{R}_{\geq 0}$ and $f_L \in \mathbb{R}_{\geq 0}$, respectively. The link actuator is fixed to the moving platform in the proximity of O_C and is used to control l and f_L in a coordinated action with the

[1] For generality we consider both positive and negative thrust. Although aerial vehicles can usually provide only positive thrust, actually, the variable pitch solution can provide negative thrust as well. However, if only positive thrust is allowed, our controller is still valid, since this constraint can be meet in the planning phase as explained later in the paper.

[2] $\mathsf{S}^2 = \{\mathbf{v} \in \mathbb{R}^3 | \ \|\mathbf{v}\| = 1\}$.

[3] We express the link orientation in $\mathcal{F}_C$ because the goal is to control the aerial vehicle position relative to the moving platform rather than to $\mathcal{F}_W$.

aerial vehicle thrust force. We recall from Sect. 3.3.2 that the link actuator exerts an input torque $\tau_W \in \mathbb{R}$ that controls the link length. The constant rotational inertia and constant radius of the link actuator are denoted by $J_W \in \mathbb{R}_{>0}$ and $r_W \in \mathbb{R}_{>0}$, respectively.

Since the link is attached to the aerial vehicle center of mass by a passive rotational joint, the aerial vehicle rotational dynamics is independent from the translational dynamics and it is equal to the one derived in Sect. 3.2:

$$\dot{\mathbf{R}}_R = \mathbf{R}_R \boldsymbol{\Omega}_R \tag{4.2}$$

$$\mathbf{J}_R \dot{\boldsymbol{\omega}}_R = \mathbf{J}_R \boldsymbol{\omega}_R \times \boldsymbol{\omega}_R + \boldsymbol{\tau}_R. \tag{4.3}$$

The linear velocity of the aerial vehicle is obtained differentiating $\mathbf{p}_R^W = \mathbf{p}_C^W + l\mathbf{R}_C\mathbf{d}^C$:

$$\dot{\mathbf{p}}_R^W = \mathbf{R}_C \left(\dot{\mathbf{p}}_C^C + l\boldsymbol{\Omega}_C \mathbf{d}^C + \dot{l}\mathbf{d}^C + l\dot{\mathbf{d}}^C \right). \tag{4.4}$$

To derive the dynamic equations of the generalized coordinates $\mathbf{q} = [l \ \varphi \ \delta]^\top$ we use the Newton-Euler approach,[4] solving the balance of the forces acting on O_R in $\mathcal{F}_W$, and the balance of momenta about the axis of the link actuator (see Sect. 3.3.2):

$$m_R \ddot{\mathbf{p}}_R^W = -f_L \mathbf{R}_C \mathbf{d}^C - f_R \mathbf{z}_R^W - m_R g \mathbf{z}_W^W \tag{4.5}$$

$$\bar{J}_W \ddot{l} = \bar{\tau}_W + f_L, \tag{4.6}$$

where $\bar{J}_W = J_W / r_W^2$, $\bar{\tau}_W = \tau_W / r_W$. The acceleration $\ddot{\mathbf{p}}_R^W$ is obtained by further differentiating (4.4), i.e.,

$$\ddot{\mathbf{p}}_R^W = \mathbf{R}_C [\bar{\mathbf{a}}_x + \mathbf{J}_\mathbf{q} \ddot{\mathbf{q}}], \tag{4.7}$$

where $\bar{\mathbf{a}}_x = \boldsymbol{\Omega}_C (\dot{\mathbf{p}}_C^C + l\boldsymbol{\Omega}_C \mathbf{d}^C + 2\mathbf{J}_\mathbf{q}\dot{\mathbf{q}}) + \ddot{\mathbf{p}}_C^C + l\dot{\boldsymbol{\Omega}}_C \mathbf{d}^C + \dot{\mathbf{J}}_\mathbf{q}\dot{\mathbf{q}}$ and

$$\mathbf{J}_\mathbf{q} = \begin{bmatrix} \cos\delta\cos\varphi & -l\cos\delta\sin\varphi & -l\cos\varphi\sin\delta \\ -\sin\delta & 0 & -l\cos\delta \\ \cos\delta\sin\varphi & l\cos\delta\cos\varphi & -l\sin\delta\sin\varphi \end{bmatrix}. \tag{4.8}$$

Replacing (4.7) into (4.5) and after some algebra we get

$$m_R \mathbf{J}_\mathbf{q} \ddot{\mathbf{q}} + f_L \mathbf{d}^C = -\underbrace{m_R \bar{\mathbf{a}}_x}_{\mathbf{a}_x} - \underbrace{m_R g \mathbf{R}_C^\top \mathbf{e}_3}_{\mathbf{a}_g} - \underbrace{f_R \mathbf{R}_C^\top \mathbf{R}_R \mathbf{e}_3}_{\mathbf{a}_{f_R}}, \tag{4.9}$$

[4] Since one of our goal is the one of controlling the internal force along the link, it results helpful to have its analytical expression. Newton-Euler is then the proper method to use as explained in Sect. 2.1. Indeed, using the Lagrangian formalism, we would not have obtained the sought internal force expression.

Finally, gathering (4.9) and (4.6) we obtain a square system

$$\underbrace{\begin{bmatrix} m_R\mathbf{J}_\mathbf{q} & \mathbf{d}^C \\ \mathbf{J}_{W\mathbf{q}} & -1 \end{bmatrix}}_{\mathbf{W}} \begin{bmatrix} \ddot{\mathbf{q}} \\ f_L \end{bmatrix} = \underbrace{\begin{bmatrix} -\mathbf{a}_x - \mathbf{a}_g \\ 0 \end{bmatrix}}_{\mathbf{a}} + \underbrace{\begin{bmatrix} -\mathbf{a}_{f_R} \\ \bar{\tau}_W \end{bmatrix}}_{\mathbf{a_u}}, \tag{4.10}$$

where $\mathbf{J}_{W\mathbf{q}} = [\bar{J}_W \ 0 \ 0] \in \mathbb{R}^{1\times 3}$ and $\mathbf{W} \in \mathbb{R}^{4\times 4}$ is invertible if and only if $l \neq 0$ and $\delta \neq \pm\pi/2$, that correspond to the singularities of the pseudo-spherical coordinates of O_R. Inverting equation (4.10) out of these singularities, we obtain

$$\ddot{\mathbf{q}} = \begin{bmatrix} \mathbf{I}_3 & \mathbf{0}_{3\times 1} \end{bmatrix} \mathbf{W}^{-1}(\mathbf{a} + \mathbf{a_u}) = \sigma(\mathbf{x}, \mathbf{X}_C^2, \mathbf{u}) \tag{4.11}$$

$$f_L = \begin{bmatrix} \mathbf{0}_{1\times 3} & 1 \end{bmatrix} \mathbf{W}^{-1}(\mathbf{a} + \mathbf{a_u}), \tag{4.12}$$

where $\mathbf{x} = (\mathbf{q}, \dot{\mathbf{q}}, \mathbf{R}_R, \boldsymbol{\omega}_R)$ is the system state, $\mathbf{u} = [f_R \ \boldsymbol{\tau}_R^\top \ \bar{\tau}_W]^\top = [u_1 \ u_2 \ u_3 \ u_4 \ u_5]^\top$ is the vector of inputs, and

$$\mathbf{X}_C^j = (\mathbf{x}_C^0, \mathbf{x}_C^1, \ldots, \mathbf{x}_C^j) \text{ for } j \in \mathbb{N}_{>0}, \tag{4.13}$$

with

$$\begin{aligned} \mathbf{x}_C^i &= (\mathbf{v}_C^{C(i-1)}, \boldsymbol{\omega}_C^{(i-1)}) \text{ for } i = 1, 2, \ldots \\ \mathbf{x}_C^0 &= (\mathbf{p}_C^W, \mathbf{R}_C) \end{aligned} \tag{4.14}$$

where $\mathbf{v}_C^C = \mathbf{R}_C^\top \frac{d\mathbf{p}_C}{dt}$. $\mathbf{X}_C^j$ in (4.13) gathers the terms related to the motion of the platform.

Gathering Eqs. (4.2), (4.3) and (4.11) we have a complete description of the system dynamics:

$$\ddot{\mathbf{q}} = \begin{bmatrix} \mathbf{I}_3 & \mathbf{0}_{3\times 1} \end{bmatrix} \mathbf{W}^{-1}(\mathbf{a} + \mathbf{a_u}) = \sigma(\mathbf{x}, \mathbf{X}_C^2, \mathbf{u}) \tag{4.15a}$$

$$\dot{\mathbf{R}}_R = \mathbf{R}_R \boldsymbol{\Omega}_R \tag{4.15b}$$

$$\mathbf{J}_R \dot{\boldsymbol{\omega}}_R = \mathbf{J}_R \boldsymbol{\omega}_R \times \boldsymbol{\omega}_R + \boldsymbol{\tau}_R. \tag{4.15c}$$

In the following we show some results that apply to simpler and yet relevant cases of the generic system considered so far. It is then useful to show how we can particularize (4.15) for those cases:

- *Fixed platform*: one can simply set $\mathbf{x}_C^i = (\mathbf{p}_C^{C(i)}, \boldsymbol{\omega}_C^{(i-1)}) = (\mathbf{0}, \mathbf{0})$ for all $i \geq 1$.
- *Fixed link length*: this represents the case in which there is no link actuator and the aerial vehicle is tethered directly to the platform by a link with a constant length, l. The model can be easily adapted considering all the time derivatives of l equal to zero, i.e., $\dot{l} = \ddot{l} = \ldots = 0$. In this case l becomes a parameter and the generalized coordinates reduce to $\mathbf{q} = [\varphi \ \delta]^\top$. The dynamics can be easily derived from (4.10)

considering only the first three row and $\ddot{l} = 0$. The last row is always verified since $\bar{\tau}_W$ represents the reaction force of the anchoring point.

- *Passive link actuator*: The link actuator is considered passive because a non-controllable constant torque $\tau'_W \in \mathbb{R}$ is applied along the longitudinal axis of the cylinder ($\tau_W(t) = \tau'_W$ for all $t \in \mathbb{R}_{\geq 0}$), e.g., generated by a simple constant torque spring. The length l can be then controlled only by the action of the thrust provided by the aerial vehicle. The choice of a passive link actuator instead of a controllable one makes the system simpler and easily portable by a human operator. On the other hand, as it will be clear in Sect. 4.6.3, the price to pay will be a reduced control authority on the variables of the system. In particular, the internal force of the link cannot be regulated to an arbitrary value while following a position trajectory. However it can be maintained within a desired bound, if the desired trajectory is well planned. For the sake of studying the feedback linearizability it is convenient to rewrite the model of the system (4.15) in the following Lagrangian form:

$$\mathbf{M}\ddot{\mathbf{q}} + \mathbf{c} + \mathbf{g} + \mathbf{n} + \mathbf{w} = \mathbf{Q}\mathbf{u}_R, \tag{4.16}$$

where, $\mathbf{u}_R = [u_1 \ \mathbf{u}_2^\top]^\top = [f_R \ \boldsymbol{\tau}_R^\top]^\top \in \mathbb{R}^4$ is the reduce input vector, $\mathbf{M}(\mathbf{q}) \in \mathbb{R}^{3\times 3}$ is the positive definite inertia matrix, $\mathbf{c}(\mathbf{q}, \dot{\mathbf{q}}, \dot{\mathbf{p}}_C^C, \boldsymbol{\omega}_C) \in \mathbb{R}^3$ contains all the centrifugal/Coriolis terms, $\mathbf{g}(\mathbf{q}, \mathbf{R}_C) \in \mathbb{R}^3$ contains all the gravity terms, $\mathbf{n}(\mathbf{q}, \ddot{\mathbf{p}}_C^C, \dot{\boldsymbol{\omega}}_C) \in \mathbb{R}^3$ contains the terms depending on the acceleration of the moving platform, $\mathbf{w}(\tau_W) \in \mathbb{R}^3$ contains the terms depending on the constant torque winch, and $\mathbf{Q}(\mathbf{q}, \mathbf{R}_R, \mathbf{R}_C) \in \mathbb{R}^{3\times 4}$ is related to the generalized forces, referred as $\mathbf{a}_\mathbf{u}$, performing work on $\mathbf{q}$, such that

$$\mathbf{a}_\mathbf{u} = \mathbf{Q}(\mathbf{q}, \mathbf{R}_R, \mathbf{R}_C)\mathbf{u} = [-\mathbf{J}_\mathbf{q}^\top \mathbf{R}_C^\top \mathbf{R}_R \mathbf{e}_3 \ \ \mathbf{0}_{3\times 3}]\mathbf{u}_R, \tag{4.17}$$

For sake of brevity we do not report here the full expression of each term. Notice that in Lagrangian representation of the dynamics the internal force of the link does not appear, differently from (4.11) and (4.12). This is useful since, as it will be clear in Sect. 4.6.3, the internal force along the link is not part of the differential flat/feedback linearizing output for the tethered system with passive link actuator.

- *Reduced model*: in the following Sect. 4.8 we shall show some particular results proven only in the particular case in which the link length and the ground platform are fixed, and the vehicle is restricted to move on a 2D vertical plane (for simplicity let us consider the plane $(\mathbf{x}_W, \mathbf{z}_W)$). To write the dynamics of the system in this particular conditions starting from the previous model, we first parametrize the vehicle attitude by the *Euler-angles* roll, pitch and yaw, (ϕ, θ, ψ), being the angles of rotation about the major axes $(\mathbf{x}_R, \mathbf{y}_R, \mathbf{z}_R)$. We then impose $\phi, \psi = 0$ that implies $\mathbf{y}_R = \mathbf{y}_W$. Furthermore we can consider the azimuth constantly to zero, i.e., $\delta = \dot{\delta} = \ddot{\delta} = 0$. Under this conditions the system degrees of freedom reduce to two, described by the new vector $\mathbf{q}' = [\varphi \ \ \theta]^\top \in \mathbb{R}^2$, actuated by the total thrust and the torque about $\mathbf{y}_R$, $\mathbf{u}' = [u_1 \ \ u_3]^\top = [f_R \ \ \tau_{Ry}]^\top \in \mathbb{R}^2$. Under those assumptions and definitions, we can rewrite (4.15) as:

Table 4.3 Particular cases of the general tethered aerial system and corresponding dynamics

Particular cases	Dynamics
Static platform	(4.15) with $\mathbf{x}_C^i = (\mathbf{p}_C^{C(i)}, \boldsymbol{\omega}_C^{(i-1)}) = (\mathbf{0}, \mathbf{0})$ for all $i \geq 1$
No link actuator	(4.10) with $\dot{l} = \ddot{l} = \ldots = 0$ and $\bar{\tau}_W = f_L$
Passive link actuator	(4.15) with $\tau_W = \tau'_W$ constantly
Reduced model	(4.18) with $\mathbf{q}' = [\varphi \ \theta]^\top$ and $\mathbf{u}' = [u_1 \ u_3]^\top = [f_R \ \tau_{Ry}]^\top$

$$\mathbf{M}'(\mathbf{q}')\ddot{\mathbf{q}}' + \mathbf{g}'(\mathbf{q}') = \mathbf{Q}'(\mathbf{q}')\mathbf{u}', \tag{4.18}$$

where

$$\mathbf{M}' = \begin{bmatrix} m_R l^2 & 0 \\ 0 & J_{R22} \end{bmatrix}, \quad \mathbf{g}' = \begin{bmatrix} m_R l g \mathbf{d}^\perp \cdot \mathbf{e}_3 \\ 0 \end{bmatrix},$$
$$\mathbf{Q}' = \begin{bmatrix} -l\mathbf{R}_R\mathbf{e}_3 \cdot \mathbf{d}^\perp & 0 \\ 0 & 1 \end{bmatrix}, \quad \mathbf{u}' = \begin{bmatrix} f_R \\ \tau_{Ry} \end{bmatrix} = \begin{bmatrix} u_1 \\ u_3 \end{bmatrix},$$

and J_{Rkm} with $k, m \in \{1, 2, 3\}$ corresponds to the element of the matrix $\mathbf{J}_R$ in position k, m, $\mathbf{d} = [\cos(\varphi) \ \ 0 \ \ \sin(\varphi)]^\top$, $\mathbf{d}^\perp = [-\sin(\varphi) \ \ 0 \ \ \cos(\varphi)]^\top$.

Table 4.3 gathers all the previous particular cases and the corresponding dynamics.

4.4 Differential Flatness

We recall from Sect. 2.2 that a system is *differentially flat* when it exists (at least) an output, called *flat output*, such that the states and the inputs can be expressed as an algebraic function of the flat output and its derivatives, up to a finite order [18]. Thus the flatness property would fulfill our first objective, i.e., compute analytically and offline the nominal state and input of the system required to exactly track a desired output trajectory. In fact, this property is commonly used for control to compute the feed-forward terms, and for planning and optimization to generate feasible trajectories, especially for nonholonomic and underactuated systems, considering the input limitations. Furthermore, the differential flatness property tells a lot about which are the independently controllable outputs and which is the required degree of smoothness for the corresponding desired trajectories.

For an unidirectional-thrust aerial vehicle, it is well known that the position of its CoM, $\mathbf{p}_R$, and the rotation along the $\mathbf{z}_R$ axis, ψ, (called yaw angle when using

the Euler-angles parametrization, see Sect. 2.1.3) are differentially flat outputs[5] [19, 20].

If we tether the aerial vehicle to a fixed point by a link with constant length, the link constraints the vehicle to fly on a sphere. Intuitively, the vehicle can still control the position on the sphere (two d.o.f.) and the yaw angle, but not the position along the longitudinal axis of the link. Indeed, every force component applied along this axis will not produce motion due to the kinematic constraint. On the other hand, it will stretch or compress the link, according to its direction. In other words, the vehicle cannot change the distance from the anchoring point but it can control the intensity of the internal force along the link. If then the link length is actuated, the link actuator can control its length and in thus the distance of the vehicle from the anchoring point. This intuition tell us that the output $\mathbf{y}^a = [y_1^a \ y_2^a \ y_3^a \ y_4^a \ y_5^a]^\top = [l \ \varphi \ \delta \ f_L \ \eta_i]^\top \in \mathbb{R}^5$, where η_i is a more "generalized" yaw angle (see the following) is a differentially flat output. We shall prove this result in Sect. 4.4.1.

Furthermore, let us consider for simplicity the system constrained to move on a 2D vertical plane. It is easy to notice that the link internal force and the angle between the thrust and the horizon, defined by $\vartheta_A \in \mathbb{R}$ (see later for the formal definition), are directly connected. Indeed the higher the internal force, the more the thrust tends to be parallel to the link axis, i.e., ϑ_A tends to φ. This second intuition makes us believe that the output $\mathbf{y}^b = [y_1^b \ y_2^b \ y_3^b \ y_4^b \ y_5^b]^\top = [l \ \varphi \ \delta \ \vartheta_A \ \eta_i]^\top \in \mathbb{R}^5$ is a differentially flat output as well. We shall prove this result in Sect. 4.4.2.

To prove the differential flatness we show how to express $\mathbf{x}$ and $\mathbf{u}$ as function of $\mathbf{y}^a$ or $\mathbf{y}^b$ and some of their relative derivatives, in the standard case in which η_i is the yaw angle. We recall that the state consists of the parametrization of $\mathbf{d}^C$, its velocity, the attitude of the aerial vehicle and its angular velocity, while the inputs are the thrust, the total torque provided by the robot and the winch torque. As we already said, we suppose $\mathbf{X}_C^0$ and its derivatives known (see (4.13)).

4.4.1 Stress-Related Flat Output

Let us define $\mathbf{y}_1^a = [y_1^a \ y_2^a \ y_3^a]^\top = [l \ \varphi \ \delta]^\top$ such that $\mathbf{y}^a = [\mathbf{y}_1^{a\top} \ y_4^a \ y_5^a]^\top = [\mathbf{q}^\top \ f_L \ \eta_i]^\top$. We have directly that

$$\mathbf{q} = \mathbf{y}_1^a, \quad \dot{\mathbf{q}} = \dot{\mathbf{y}}_1^a. \tag{4.19}$$

Then, from (4.6) we obtain the expression of $\bar{\tau}_W$

$$\bar{\tau}_W = \bar{J}_W \ddot{y}_1^a - y_4^a = f_1(\ddot{y}_1^a, y_4^a). \tag{4.20}$$

In order to find the expression of the missing states and inputs, one can notice that from (4.7) the linear acceleration of the aerial vehicle can be written as function of

[5] And thus also dynamic feedback linearizing outputs.

$\mathbf{y}_1^a, \dot{\mathbf{y}}_1^a, \ddot{\mathbf{y}}_1^a$, the linear velocity of the platform, its rotation and their time derivatives, i.e., $\ddot{\mathbf{p}}_R^W = \ddot{\mathbf{p}}_R^W(\mathbf{y}_1^a, \dot{\mathbf{y}}_1^a, \ddot{\mathbf{y}}_1^a, \mathbf{X}_C^2)$. Then, from (4.5), we can write the thrust vector as function of only the outputs, their derivatives and known quantities related to the trajectory of the moving platform, indeed:

$$\begin{aligned} f_R \mathbf{R}_R \mathbf{e}_3 &= -m_R \ddot{\mathbf{p}}_R^W(\mathbf{y}_1^a, \dot{\mathbf{y}}_1^a, \ddot{\mathbf{y}}_1^a, \mathbf{X}_C^2) - y_4 \mathbf{R}_C \mathbf{d}^C(\mathbf{y}_1) - m_R g \mathbf{e}_3 \\ &= \mathbf{f}_2(\mathbf{y}_1^a, \dot{\mathbf{y}}_1^a, \ddot{\mathbf{y}}_1^a, y_4, \mathbf{X}_C^2). \end{aligned} \tag{4.21}$$

Then, exploiting y_5, one can apply the same method presented in [20] in order to obtain the attitude of the aerial vehicle, its angular velocity and the total provided torque. For the sake of brevity we omit here the full re-derivation of all these functions.

Proposition *The model (4.15), is differentially flat with respect to the flat output* $\mathbf{y}^a = [l \;\; \varphi \;\; \delta \;\; f_L \;\; \eta_i]^\top$ *where* η_i *is the yaw angle of* $\mathbf{R}_R$*. In other words, the state and the inputs can be written as algebraic function of* $\mathbf{y}^a$ *and a finite number of its derivatives:*

$$\mathbf{x} = \mathbf{f}_\mathbf{x}^a(\mathbf{y}^a, \ldots, \mathbf{y}^{a(4)}, \mathbf{X}_C^2) \tag{4.22}$$

$$\mathbf{u} = \mathbf{f}_\mathbf{u}^a(\mathbf{y}^a, \ldots, \mathbf{y}^{a(4)}, \mathbf{X}_C^2). \tag{4.23}$$

4.4.2 Attitude-Related Flat Output

Firstly, we have to properly define ϑ_A in the 3D environment. Let us define a new reference frame, $\mathcal{F}_L$ centered in $\mathbf{p}_C$ and with axes $\{\mathbf{x}_L, \mathbf{y}_L, \mathbf{z}_L\}$ such that:

$$\mathbf{z}_L = \mathbf{z}_W, \quad \mathbf{y}_L = \frac{\mathbf{z}_L \times \mathbf{d}}{\|\mathbf{z}_L \times \mathbf{d}\|}, \quad \mathbf{x}_L = \mathbf{y}_L \times \mathbf{z}_L. \tag{4.24}$$

If $\mathbf{d}$ is parallel to $\mathbf{z}_W$, one can choose any arbitrary $\mathbf{y}_L$. For example, if the aerial vehicle is moving such that $\mathbf{d}$ is parallel to $\mathbf{z}_W$ at a certain time t_i, during that instant we can simply keep $\mathbf{y}_L$ constant. Practically, starting from a non singular condition, one would define a certain threshold $\epsilon \in \mathbb{R}_{>0}$ such that if $\|\mathbf{z}_W \times \mathbf{d}\| < \epsilon$, $\mathbf{y}_L$ is kept constant. In particular we can define the vertical plane $\mathcal{P}_L$ that includes $\mathbf{d}$, i.e., $\mathcal{P}_L = \{\mathbf{v} \in \mathbb{R}^3 \mid \exists \lambda_1, \lambda_2 \in \mathbb{R} \;:\; \mathbf{v} = \lambda_1 \mathbf{x}_L + \lambda_2 \mathbf{z}_L\}$; and the projection of $-\mathbf{z}_R$ into $\mathcal{P}_L$ defined by:

$$\boldsymbol{\alpha} = [\alpha_1 \;\; \alpha_2 \;\; \alpha_3]^\top = -\mathbf{P}_L \mathbf{z}_R, \tag{4.25}$$

where $\mathbf{P}_L = [\mathbf{x}_L \;\; \mathbf{0} \;\; \mathbf{z}_L]^\top \in \mathbb{R}^{3\times 3}$ is the projector on $\mathcal{P}_L$, with respect to $\mathcal{F}_L$. Finally we define ϑ_A as the angle between $\boldsymbol{\alpha}$ and $\mathbf{z}_L$:

$$\vartheta_A = \text{atan2}\,(\alpha_1, \alpha_3) = \text{atan2}\left(-\mathbf{e}_1^\top \mathbf{P}_L \mathbf{z}_R, -\mathbf{e}_3^\top \mathbf{P}_L \mathbf{z}_R\right). \tag{4.26}$$

Figure 4.2 shows how ϑ_A is graphically defined.

In order to demonstrate that $\mathbf{y}^b$ is also a flat output we show that there exists a bijective map between $\mathbf{y}^b$ and $\mathbf{y}^a$. Considering $\mathbf{X}_C^2$ (see 4.13) as a known input, the map from $\mathbf{y}^a$ to $\mathbf{y}^b$ and their derivatives, i.e., $(\mathbf{y}^b, \ldots, \mathbf{y}^{b(4)}) = \mathbf{g}_b(\mathbf{y}^a, \ldots, \mathbf{y}^{a(4)}, \mathbf{X}_C^2)$ is simply given by the flatness of the system w.r.t. $\mathbf{y}^a$. In fact, given $\mathbf{y}^a$ and its derivatives, one can compute the nominal state and inputs with (4.22) and (4.23). Then, from Eq. (4.26), it is easy to compute $\mathbf{y}^b$ and the relative derivatives.

Regarding the opposite sense of the map, i.e., from $\mathbf{y}^b$ to $\mathbf{y}^a$:

$$(\mathbf{y}^a, \ldots, \mathbf{y}^{a(4)}) = \mathbf{g}_a(\mathbf{y}^b, \ldots, \mathbf{y}^{b(4)}, \mathbf{X}_C^2), \tag{4.27}$$

the map is immediate for $\mathbf{q}$ and ψ. Let us define $\mathbf{y}_1^b = [y_1^b \;\; y_2^b \;\; y_3^b]^\top = [l \;\; \varphi \;\; \delta]^\top$ such that $\mathbf{y}^b = [\mathbf{y}_1^{b\top} \;\; y_4^b \;\; y_5^b]^\top = [\mathbf{q}^\top \;\; \vartheta_A \;\; \eta_l]^\top$. We have that $\mathbf{y}_1^a = \mathbf{y}_1^b$ and $y_5^a = y_5^b$. Then we can retrieve f_L, and so y_4^a, from $\mathbf{y}^b$ and its derivatives projecting both sides of (4.5) on the plane $\mathcal{P}_L$. Not considering the second equations (always zero), after some algebra we can obtain:

$$y_4^a = f_L = -m_R[0 \;\; 1]^\top \mathbf{T}^{-1}[\mathbf{e}_1 \;\; \mathbf{e}_3]^\top \mathbf{P}_L(\ddot{\mathbf{p}}_R + g\mathbf{z}_W), \tag{4.28}$$

where $\mathbf{T}(\mathbf{y}^b) = [\mathbf{e}_1 \;\; \mathbf{e}_3]^\top [\mathbf{P}_L \mathbf{z}_R \;\; \mathbf{P}_L \mathbf{d}]$ is invertible if and only if $\mathbf{z}_R \not\perp \mathcal{P}_L$ and $\mathbf{P}_L \mathbf{z}_R \nparallel \mathbf{P}_L \mathbf{d}$. Finally, to retrieve the derivatives of f_L one can simply differentiate (4.28) w.r.t. time. This proves that between $\mathbf{y}^a$ and $\mathbf{y}^b$, and their derivatives, there is a bijective map.

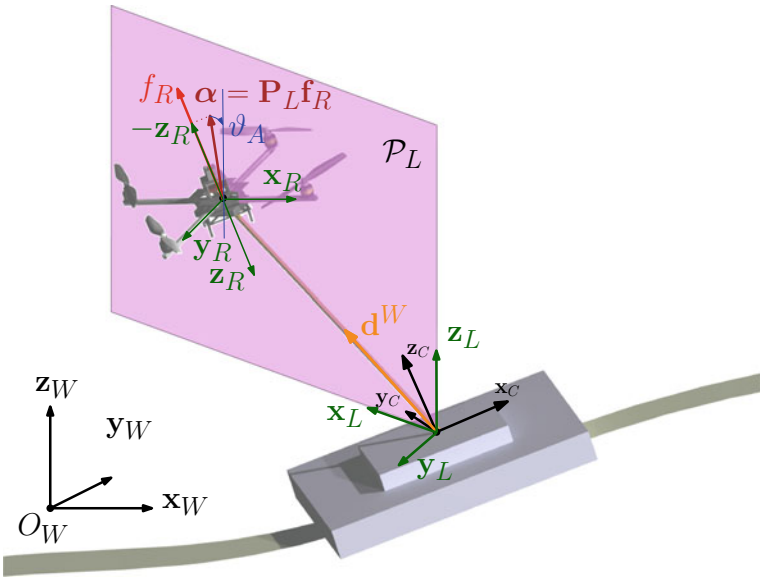

Fig. 4.2 Visual description of the angle ϑ_A

Combining (4.22), (4.23) and (4.27), state and inputs of the system can be written as an algebraic function of $\mathbf{y}^b$ its derivatives, and the known quantity $\mathbf{X}_C^2$, proving that $\mathbf{y}^b$ is a flat output:

$$\mathbf{x} = \mathbf{f}_{\mathbf{x}}^a(\mathbf{g}_a(\mathbf{y}^b, \ldots, \mathbf{y}^{b(4)}, \mathbf{X}_C^2), \mathbf{X}_C^2) = \mathbf{f}_{\mathbf{x}}^b(\mathbf{y}^b, \ldots, \mathbf{y}^{b(4)}, \mathbf{X}_C^2) \tag{4.29}$$

$$\mathbf{u} = \mathbf{f}_{\mathbf{u}}^a(\mathbf{g}_a(\mathbf{y}^b, \ldots, \mathbf{y}^{b(4)}, \mathbf{X}_C^2), \mathbf{X}_C^2) = \mathbf{f}_{\mathbf{u}}^b(\mathbf{y}^b, \ldots, \mathbf{y}^{b(4)}, \mathbf{X}_C^2). \tag{4.30}$$

Proposition *The model (4.15), is differentially flat with respect to the flat output* $\mathbf{y}^b = [l \;\; \varphi \;\; \delta \;\; \vartheta_A \;\; \eta_i]^\top$ *where* η_i *is the yaw angle of* $\mathbf{R}_R$*. In other words, the state and the inputs can be written as algebraic function of* $\mathbf{y}^b$ *and a finite number of its derivatives, i.e., Eqs. (4.29) and (4.30).* □

4.4.3 Differential Flatness for Passive Link Actuator

Let us define $\mathbf{y}^c = [\mathbf{y}_1^{c\top} \;\; y_4^c]^\top = [\mathbf{q}^\top \;\; \eta_i]^\top \in \mathbb{R}^4$. Part of the state is directly given by $\mathbf{y}_1^c$, i.e., $\mathbf{q} = \mathbf{y}_1^c$, $\dot{\mathbf{q}} = \dot{\mathbf{y}}_1^c$. Only the part of the state related to the rotational dynamics and the inputs have still to be derived. From (4.6) we can write the internal force as function of $\ddot{\mathbf{y}}_1^c$:

$$f_L = \bar{J}_W \ddot{l} - \bar{\tau}_W = f_L(\ddot{\mathbf{y}}_1^c). \tag{4.31}$$

Then, it is exactly the same procedure as in Sect. 4.4.1. One can write $\mathbf{y}_1^a = \mathbf{y}_1^c$, $y_4^a = f_L(\ddot{\mathbf{y}}_1^c)$, $y_5^a = y_5^c$, and then use (4.22) and (4.23) to compute nominal state and input.

Proposition *The model (4.2), (4.3) and (4.16), is differentially flat with respect to the flat output* $\mathbf{y}^c = [l \;\; \varphi \;\; \delta \;\; \eta_i]^\top$ *where* η_i *is the yaw angle of* $\mathbf{R}_R$*. In other words the state and the inputs can be written as algebraic function of* $\mathbf{y}^c$ *and a finite number of its derivatives.*

$$\mathbf{x} = \mathbf{f}_{\mathbf{x}}^c(\mathbf{y}^c, \ldots, \mathbf{y}^{c(4)}, \mathbf{X}_C^2) \tag{4.32}$$

$$\mathbf{u} = \mathbf{f}_{\mathbf{u}}^c(\mathbf{y}^c, \ldots, \mathbf{y}^{c(4)}, \mathbf{X}_C^2). \tag{4.33}$$

4.4.3.1 Discussion on Link Internal Force Regulation

We already remarked that, differently from the active link actuator case, the internal force along the link is not part of the flat output for this system. This means that its value cannot be directly controlled. On the contrary, from (4.31), it is a byproduct of the desired output trajectory, and in particular of the desired link length acceleration. Nevertheless, in order to keep the internal force always within a desired bound $\mathcal{B}_{f_L} = [\underline{f_L}, \overline{f_L}]$ where $\underline{f_L}, \overline{f_L} \in \mathbb{R}$, we can exploit the flatness of the system to design

suitable desired trajectories of $\mathbf{y}^c$. In particular, from Eq. (4.31) we have that $f_L \in \mathcal{B}_{f_L}$ if and only if $\ddot{l} \in \mathcal{B}_{\ddot{l}} = [\underline{\ddot{l}}, \bar{\ddot{l}}]$ where $\bar{\ddot{l}} = (\bar{\tau}'_W + \overline{f_L})/\bar{J}_W$ and $\underline{\ddot{l}} = (\bar{\tau}'_W + \underline{f_L})/\bar{J}_W$. In other words the constraint on the internal force can be translated using the flatness into a constraint on the desired trajectory of l.

Notice that the steady configuration, $\ddot{l} = 0$, belongs to $\mathcal{B}_{\ddot{l}}$ if and only if $\underline{\ddot{l}} \leq 0 \leq \bar{\ddot{l}}$ that in turn means $-\overline{f_L} \leq \bar{\tau}'_W \leq -\underline{f_L}$. In particular, if for $\ddot{l} = 0$ we want a desired internal force value $f_L{}^\star \in \mathcal{B}_{f_L}$, we have to design the passive link actuator such that $\bar{\tau}'_W = \tau'_W / r_W = -f_L{}^\star$. Another parameter of the link actuator that can be optimized is its inertia $\bar{J}_W$. Indeed it affects how $\mathcal{B}_{f_L}$ is mapped on $\mathcal{B}_{\ddot{l}}$, e.g., if we make $\bar{J}_W$ small enough, big variations of $\ddot{l}$ imply small variations of the internal force and thus an almost constant internal force, $f_L \approx f_L{}^\star$.

4.5 Hierarchical Control

In this section we exploit the previously proven flatness in order to design a controller based on a hierarchical method. This is very common for the control of aerial vehicles because it allows to separate the control of the attitude from the one of the translational dynamics. This is convenient especially for commercial available platforms for which one cannot directly control the spinning velocity of the propellers. Often, one can only control the angular velocity or the attitude of the vehicle, sending the desired Euler angles. Then, internally to the platform, a closed low level controller track the desired references.

To cope with these problems, we propose a simpler control strategy, based on hierarchical techniques, that can be easily implemented in every platform. Indeed, thanks to the separation between outer loop (normally position control) and inner loop (attitude control) controls, one can easily adapt the proposed controller to the specific platform functionalities. Similar techniques were successfully implemented and tested in, e.g., [5, 6], to only stabilize the position of the vehicle. However, those methods cannot be directly applied to solve our problem because they are designed for different systems, although similar.

The validity of the method has been proven experimentally. The related results are shown in Sect. 5.2.

4.5.1 Force-Related Hierarchical Control

In the following we design a hierarchical controller for controlling the output $\mathbf{y}^a$, namely the position of the aerial vehicle and the internal force along the link. The controller is based on the cascaded structure between the translational and rotational dynamics.

Given a desired position trajectory $\mathbf{p}_R^C(t)$, defined in terms of the generalized coordinates $\mathbf{y}_1^{ad}(t) = \mathbf{q}(t)^d$ we define

$$\ddot{\mathbf{q}}^\star = \ddot{\mathbf{q}}^d + \mathbf{K}_\mathbf{q}^D(\dot{\mathbf{q}}^d - \dot{\mathbf{q}}) + \mathbf{K}_\mathbf{q}^P(\dot{\mathbf{q}}^d - \dot{\mathbf{q}}), \tag{4.34}$$

where $\mathbf{K}_\mathbf{q}^P, \mathbf{K}_\mathbf{q}^D \in \mathbb{R}^{3\times3}_{>0}$ are diagonal matrices. The vector $\ddot{\mathbf{q}}^\star$ could be seen as the desired acceleration that lets $\mathbf{q}$ follow the desired trajectory $\mathbf{q}^d(t)$ using a PD strategy. In case of model uncertainties or disturbances one can add an integral term as well.

Then, given a desired trajectory for the internal force of the link $y_4^a = f_L(t)^d$, and inverting the balance of momenta on the link actuator (4.6), we compute the link actuator torque as

$$\bar{\tau}_W = \bar{J}_W \ddot{l}^\star - {f_L}^d. \tag{4.35}$$

To finally implement $\ddot{\mathbf{q}}^\star$ we compute the desired thrust vector inverting the balance force equation on O_R (4.5), like for the flatness computation in (4.21)

$$\mathbf{f}_R^\star = f_R \mathbf{R}_R^\star \mathbf{e}_3 = \mathbf{R}_C(-\mathbf{a}_x - \mathbf{a}_g - {f_L}^d \mathbf{d}^C - m_R \mathbf{J}_\mathbf{q} \ddot{\mathbf{q}}^\star). \tag{4.36}$$

From the desired thrust vector we derive the input f_R as

$$f_R = \left\| -\mathbf{a}_x - \mathbf{a}_g - {f_L}^d \mathbf{d}^C - m_R \mathbf{J}_\mathbf{q} \ddot{\mathbf{q}}^\star \right\|, \tag{4.37}$$

and the desired z-axis of $\mathcal{F}_R$, i.e., $\mathbf{z}_R^\star = \mathbf{R}_R^\star \mathbf{e}_3 = \mathbf{f}_R^\star / f_R$.

The desired yaw angle ψ^d together with $\mathbf{z}_R^\star$ define the desired attitude of the vehicle described by $\mathbf{R}_R^\star$. In fact, given ψ^d we define $\mathbf{x}_R' = \mathbf{R}_\mathbf{z}(\psi^d)\mathbf{e}_1$ where $\mathbf{R}_\mathbf{z}(\psi^d)$ is the rotation matrix describing the rotation of ψ^d around $\mathbf{z}_W$. The axis $\mathbf{x}_R'$ represents the desired heading of the aerial vehicle. The desired attitude is computed creating an orthonormal basis using the vectors $\mathbf{x}_R'$ and $\mathbf{z}_R^\star$ that is given by $\mathbf{R}_R^\star = [\mathbf{x}_R^\star \ \mathbf{y}_R^\star \ \mathbf{z}_R^\star]$ where,

$$\mathbf{y}_R^\star = \frac{\mathbf{z}_R^\star \times \mathbf{x}_R'}{\left\| \mathbf{z}_R^\star \times \mathbf{x}_R' \right\|}, \qquad \mathbf{x}_R^\star = \frac{\mathbf{y}_R^\star \times \mathbf{z}_R\star}{\left\| \mathbf{y}_R^\star \times \mathbf{z}_R\star \right\|}. \tag{4.38}$$

This concludes the design of the outer loop control. Given the tracking error it computes the desired link actuator torque $\bar{\tau}_W$, the desired thrust intensity f_R and the desired attitude $\mathbf{R}_R^\star$.

If the considered platform accept as input the desired attitude and thrust, we can simply send the previous quantities as control commands. If instead the platform is controlled in thrust/angular velocity or thrust/torque, we shall show the design of an inner loop control that computes the desired angular velocity, $\boldsymbol{\omega}_R^\star$, or the desired torque, $\boldsymbol{\tau}_R$, respectively, in order to track the desired attitude computed by the outer loop control.

Let us define the attitude error [21] by the vector $\mathbf{e}_R \in \mathbb{R}^3$, computed as

$$[\mathbf{e}_R]_\times = -\frac{1}{2}(\mathbf{R}_R^{\star\top}\mathbf{R}_R - \mathbf{R}_R^\top\mathbf{R}_R^\star), \tag{4.39}$$

where $[\mathbf{e}_R]_\times$ corresponds to the skew symmetric matrix relative to $\mathbf{e}_R$. In order to steer $\mathbf{e}_R$ to zero, if the vehicle is controlled in angular velocity, we compute the desired angular velocity based on a P controller,

$$\boldsymbol{\omega}_R^\star = \boldsymbol{\omega}_R^d + \mathbf{K}_\omega^P \mathbf{e}_R, \tag{4.40}$$

where $\mathbf{K}_\omega^P \in \mathbb{R}^{3\times3}_{>0}$ is a diagonal matrix. If instead the vehicle is controlled in torque we first define the desired angular acceleration based on a PD controller,

$$\dot{\boldsymbol{\omega}}_R^\star = \dot{\boldsymbol{\omega}}_R^d + \mathbf{K}_\omega^D(\boldsymbol{\omega}_R^d - \boldsymbol{\omega}_R) + \mathbf{K}_\omega^P \mathbf{e}_R, \tag{4.41}$$

where $\mathbf{K}_\omega^D \in \mathbb{R}^{3\times3}_{>0}$ is a diagonal matrix, and $\boldsymbol{\omega}_R^d$ and $\dot{\boldsymbol{\omega}}_R^d$ are the nominal angular velocity and acceleration, respectively, computed by the flatness from the desired output trajectory as in Sect. 4.4.1. Inverting the rotational dynamics we can finally find the input torque $\boldsymbol{\tau}_R$,

$$\boldsymbol{\tau}_R = -\mathbf{J}_R\boldsymbol{\omega}_R \times \boldsymbol{\omega}_R + \mathbf{J}_R\dot{\boldsymbol{\omega}}_R^\star. \tag{4.42}$$

If the inner loop is sufficiently faster than the outer loop, the asymptotic convergence of $\mathbf{q}$ to $\mathbf{q}^d$ is guaranteed. Figure 4.3a shows a schematic representation of the controller $\mathbf{u} = \Gamma^a_{\text{HC}}(\mathbf{x}, \mathbf{X}_C^2, \mathbf{y}^{ad}(t))$ given by (4.35), (4.37) and (4.42).

Notice that it is easy to rewrite the controller Γ^a_{HC} for the particular cases mentioned in Sect. 4.3. For the case of a passive link actuator one can use the same controller once the nominal internal force is computed by (4.31).

4.5.2 *Attitude-Related Hierarchical Control*

For the control of $\mathbf{y}^b$ we exploit the bijection function between $\mathbf{y}^b$ and $\mathbf{y}^a$, and the previously presented hierarchical controller for the tracking of $\mathbf{y}^a$. In particular, from the desired trajectory $\mathbf{y}^{bd}(t)$, we can compute the equivalent trajectory of $\mathbf{y}^a$, i.e., $(\mathbf{y}^{ad}, \ldots, \mathbf{y}^{ad(4)}) = \mathbf{g}_a(\mathbf{y}^{bd}, \ldots, \mathbf{y}^{bd(4)}, \mathbf{X}_C^2)$. Then we apply the hierarchical controller shown before to effectively track $\mathbf{y}^{ad}(t)$. The hierarchical controller to track $\mathbf{y}^{bd}(t)$ defined by Γ^b_{HC}, is equal to:

$$\mathbf{u} = \Gamma^b_{\text{HC}}(\mathbf{x}, \mathbf{X}_C^2, \mathbf{y}^{bd}(t)) = \Gamma^a_{\text{HC}}(\mathbf{x}, \mathbf{X}_C^2, \mathbf{g}_a(\mathbf{y}^{bd}(t), \mathbf{X}_C^2)). \tag{4.43}$$

Thanks to the fact that $\mathbf{g}_a$ and $\mathbf{g}_b$ are bijective maps, if the closed loop system is able to track $\mathbf{y}^{ad}(t)$, it will implicitly track $\mathbf{y}^{bd}(t)$. Figure 4.3b shows a schematic representation of the controller.

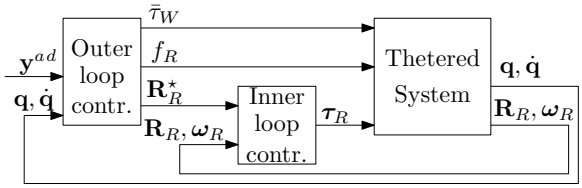

(a) Controller for $\mathbf{y}^a$

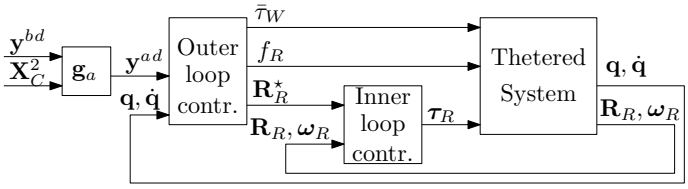

(b) Controller for $\mathbf{y}^b$

Fig. 4.3 Schematic representation of the two hierarchical controllers

4.6 Dynamic Feedback Linearization

From the theory we know that a flat output is also an exactly dynamical feedback linearizing output on an open and dense set of the state space [22]. In this section we shall design a controller based on the dynamic feedback linearization technique the problem of the exact tracking of the outputs $\mathbf{y}^a$, $\mathbf{y}^b$, and $\mathbf{y}^c$. For the problem of the exact tracking of such output we will design a controller based on the dynamic feedback linearization technique. We recall that in the following $\mathbf{x} = (\mathbf{q}, \dot{\mathbf{q}}, \mathbf{R}_R, \boldsymbol{\omega}_R)$ is the system state, $\mathbf{u} = [f_R \ \boldsymbol{\tau}_R^\top \ \bar{\tau}_W]^\top = [u_1 \ u_2 \ u_3 \ u_4 \ u_5]^\top$ is the input vector and the outputs are

(i) $\mathbf{y}^a = [y_1^a \ y_2^a \ y_3^a \ y_4^a \ y_5^a]^\top = [l \ \varphi \ \delta \ f_L \ \eta_i]^\top \in \mathbb{R}^5$,
(ii) $\mathbf{y}^b = [y_1^b \ y_2^b \ y_3^b \ y_4^b \ y_5^b]^\top = [l \ \varphi \ \delta \ \vartheta_A \ \eta_i]^\top \in \mathbb{R}^5$ and
(iii) $\mathbf{y}^c = [y_1^c \ y_2^c \ y_3^c \ y_4^c]^\top = [l \ \varphi \ \delta \ \eta_i]^\top \in \mathbb{R}^4$.

4.6.1 Force-Related Feedback Linearizing Output

In the previous sections we considered η_i as the yaw angle when the rotation of $\mathcal{F}_R$ is parametrized by the Euler angles. However, in the following we consider any generic parametrization $\boldsymbol{\eta} = [\eta_1 \ \eta_3 \ \eta_3]^\top \in \mathbb{R}^3$ of $\mathbf{R}_R$, such that $\mathbf{R}_R = \mathbf{R}_R(\boldsymbol{\eta})$ and $\dot{\boldsymbol{\eta}} = \mathbf{T}_{\boldsymbol{\eta}}\boldsymbol{\omega}_R$ where $\mathbf{T}_{\boldsymbol{\eta}}(\boldsymbol{\eta}) \in \mathbb{R}^{3\times 3}$ is given by the particular parametrization [23]. From (4.3) the dynamics of $\boldsymbol{\eta}$ is

$$\ddot{\boldsymbol{\eta}} = \underbrace{\dot{\mathbf{T}}_{\boldsymbol{\eta}}\boldsymbol{\omega}_R + \mathbf{T}_{\boldsymbol{\eta}}\mathbf{J}_R^{-1}(\mathbf{J}_R\boldsymbol{\omega}_R \times \boldsymbol{\omega}_R)}_{\mathbf{b}_{\boldsymbol{\eta}}(\boldsymbol{\eta},\dot{\boldsymbol{\eta}})} + \underbrace{[\,\mathbf{0}_{3\times1} \quad \mathbf{T}_{\boldsymbol{\eta}}\mathbf{J}_R^{-1} \quad \mathbf{0}_{3\times1}\,]}_{\mathbf{E}_{\boldsymbol{\eta}}(\boldsymbol{\eta})}\mathbf{u}. \tag{4.44}$$

Then we consider η_i as any entry of $\boldsymbol{\eta}$ such that, in the domain of interest, it holds

$$e_{\eta_i} = \frac{\partial \ddot{\eta}_i}{\partial \tau_{Rz}} = \mathbf{e}_i^\top \mathbf{T}_{\boldsymbol{\eta}}\mathbf{J}_R^{-1}\mathbf{e}_3 \neq 0. \tag{4.45}$$

For example, taking $\boldsymbol{\eta} = [\phi \;\; \theta \;\; \psi]^\top$ as the classical Roll-Pitch-Yaw parametrization of $\mathbf{R}_R$ and $\eta_i = \psi$, we have that

$$\mathbf{T}_{\boldsymbol{\eta}}(\boldsymbol{\eta}) = \begin{bmatrix} 1 & \sin\phi\tan\theta & \cos\phi\tan\theta \\ 0 & \cos\phi & -\sin\phi \\ 0 & \sin\phi\sec\theta & \cos\phi\sec\theta \end{bmatrix} \text{ and } e_{\eta_i} = \frac{1}{J_{R33}}\cos\phi\sec\theta, \tag{4.46}$$

Notice that for this choice (4.45) holds always except for $\phi = \pi/2$ and $\theta = \pi/2$.

Intuitively, only $\bar{\tau}_W$ and $\mathbf{f}_R$ play a role in the control of l, φ, δ and f_L (see (4.10)) and they are not affected by τ_{Rz}. Indeed $\mathbf{f}_R$ is not influenced by rotations along $\mathbf{z}_R$ and therefore not even by the torque τ_{Rz} acting about it. Then it is necessary to complete the set of outputs with a quantity dynamically dependent on τ_{Rz} to have a well-posed tracking problem. Thus, we recall that the output of interest is $\mathbf{y}^a = [y_1^a \;\; y_2^a \;\; y_3^a \;\; y_4^a \;\; y_5^a]^\top = [l \;\; \varphi \;\; \delta \;\; f_L \;\; \eta_i]^\top \in \mathbb{R}^5$.

Applying the feedback linearization technique (see Sect. 2.3), and recalling Eqs. (4.10) and (4.44), we immediately see that (y_1^a, y_2^a, y_3^a) have to be differentiated twice until f_R and $\bar{\tau}_W$ appear. Also y_5^a has to be differentiated twice until $\boldsymbol{\tau}_R$ appears, while y_4^a directly depends on f_R and $\bar{\tau}_W$. Defining $\bar{\mathbf{y}}_1^a = [\ddot{y}_1^a \;\; \ddot{y}_2^a \;\; \ddot{y}_3^a \;\; y_4^a]^\top$ and rearranging (4.10) and (4.44), we can write

$$\begin{bmatrix} \bar{\mathbf{y}}_1^a \\ \ddot{y}_5^a \end{bmatrix} = \begin{bmatrix} \bar{\mathbf{W}}\mathbf{a} \\ b_{\eta_i} \end{bmatrix} + \begin{bmatrix} \bar{\mathbf{W}}\mathbf{U} \\ \mathbf{e}_{\eta_i} \end{bmatrix}\mathbf{u} = \mathbf{b}(\mathbf{x}, \mathbf{X}_C^2) + \mathbf{E}(\mathbf{x}, \mathbf{X}_C^0)\mathbf{u}, \tag{4.47}$$

where $\bar{\mathbf{W}} = \mathbf{W}^{-1}$, $b_{\eta_i} = \mathbf{e}_i^\top \mathbf{b}_{\boldsymbol{\eta}}$, $\mathbf{e}_{\eta_i} = \mathbf{e}_i^\top \mathbf{E}_{\boldsymbol{\eta}}$, the vector $\mathbf{b}(\mathbf{x}, \mathbf{X}_C^2)$ gathers all the terms that do not depend on the inputs and

$$\mathbf{U} = \begin{bmatrix} -\mathbf{R}_C^\top \mathbf{R}_R \mathbf{e}_3 & \mathbf{0}_{3\times3} & \mathbf{0}_{3\times1} \\ 0 & \mathbf{0}_{1\times3} & 1 \end{bmatrix}_{4\times5} \tag{4.48}$$

$$\mathbf{E} = \begin{bmatrix} \bar{\mathbf{W}} & \mathbf{0}_{4\times1} \\ \mathbf{0}_{1\times4} & 1 \end{bmatrix} \begin{bmatrix} -\mathbf{R}_C^\top \mathbf{R}_R \mathbf{e}_3 & \mathbf{0}_{3\times3} & \mathbf{0}_{3\times1} \\ 0 & \mathbf{0}_{1\times3} & 1 \\ 0 & \mathbf{e}_i^\top \mathbf{T}_{\boldsymbol{\eta}}\mathbf{J}_R^{-1} & 0 \end{bmatrix}_{5\times5}. \tag{4.49}$$

We recall that Rearranging the rows of the decoupling matrix $\mathbf{E}$ one can notice that it is clearly singular because $\boldsymbol{\tau}_R$ does not appear in the expression of $\bar{\mathbf{y}}_1^a$.

As explained in Sect. 2.3, to obtain a full rank matrix we insert a dynamic compensator considering as new input $\bar{\mathbf{u}} = [\ddot{u}_1 \;\; u_2 \;\; u_3 \;\; u_4 \;\; \ddot{u}_5]^\top$, where $\ddot{u}_1$ and $\ddot{u}_5$ are the

second derivative of f_R and $\bar{\tau}_W$, respectively. Under this definition $\bar{\mathbf{y}}_1^a$ and y_5^a have to be differentiated twice to see the new inputs appear:

$$\begin{bmatrix} \bar{\mathbf{y}}_1^a \\ \ddot{y}_5^a \end{bmatrix} = \begin{bmatrix} \ddot{\bar{\mathbf{W}}}(\mathbf{a}+\mathbf{a}_\mathbf{u}) + 2\dot{\bar{\mathbf{W}}}(\dot{\mathbf{a}}+\dot{\mathbf{a}}_\mathbf{u}) + \bar{\mathbf{W}}(\ddot{\mathbf{a}}+\ddot{\mathbf{a}}_\mathbf{u}) \\ b_i + \mathbf{e}_{\eta_i}\bar{\mathbf{u}} \end{bmatrix}, \tag{4.50}$$

where $\ddot{\mathbf{a}}_\mathbf{u}$, after replacing the system dynamics, results:

$$\ddot{\mathbf{a}}_\mathbf{u} = \ddot{\bar{\mathbf{a}}}_\mathbf{u} + \begin{bmatrix} -u_1 \mathbf{R}_C^\top \mathbf{R}_R \left[\mathbf{J}_R^{-1}\boldsymbol{\tau}_R\right]_\times \mathbf{e}_3 - \ddot{u}_1 \mathbf{R}_C^\top \mathbf{R}_R \mathbf{e}_3 \\ \ddot{u}_5 \end{bmatrix}. \tag{4.51}$$

Since $\mathbf{J}_R$ is diagonal, i.e., $J_{Rkm} = 0$ for $k \neq m$ and $k, m \in \{1, 2, 3\}$, writing the skew symmetric matrix relative to $\mathbf{J}_R^{-1}\boldsymbol{\tau}_R$ and doing some algebra we obtain

$$\left[\mathbf{J}_R^{-1}\boldsymbol{\tau}_R\right]_\times \mathbf{e}_3 = \begin{bmatrix} -\frac{\mathbf{e}_2}{J_{R11}} & \frac{\mathbf{e}_1}{J_{R22}} & \mathbf{0}_{3\times 1} \end{bmatrix} \boldsymbol{\tau}_R. \tag{4.52}$$

Replacing Eqs. (4.52) and (4.51) into (4.50) we obtain

$$\begin{bmatrix} \ddot{\bar{\mathbf{y}}}_1^a \\ \ddot{y}_5^a \end{bmatrix} = \underbrace{\begin{bmatrix} \ddot{\bar{\mathbf{W}}}(\mathbf{a}+\mathbf{a}_\mathbf{u}) + 2\dot{\bar{\mathbf{W}}}(\dot{\mathbf{a}}+\dot{\mathbf{a}}_\mathbf{u}) + \bar{\mathbf{W}}(\ddot{\mathbf{a}}+\ddot{\bar{\mathbf{a}}}_\mathbf{u}) \\ b_i \end{bmatrix}}_{\bar{\mathbf{b}}(\bar{\mathbf{x}}, \mathbf{X}_C^4)} + \underbrace{\begin{bmatrix} \bar{\mathbf{W}}\bar{\mathbf{U}} \\ \mathbf{e}_{\eta_i} \end{bmatrix}}_{\bar{\mathbf{E}}(\bar{\mathbf{x}}, \mathbf{X}_C^0)} \bar{\mathbf{u}}, \tag{4.53}$$

where $\bar{\mathbf{U}} = \begin{bmatrix} -\mathbf{R}_C^\top \mathbf{R}_R \mathbf{T} & \mathbf{0}_{3\times 1} \\ \mathbf{0}_{1\times 4} & 1 \end{bmatrix}$, $\bar{\mathbf{x}} = (\mathbf{q}, \dot{\mathbf{q}}, \mathbf{R}_R, \boldsymbol{\omega}_R, f_R, \dot{f}_R, \bar{\tau}_W, \dot{\bar{\tau}}_W)$ is the extended state, and $\mathbf{T} = [\mathbf{e}_3 \;\; -\frac{u_1}{J_{R11}}\mathbf{e}_2 \;\; \frac{u_1}{J_{R22}}\mathbf{e}_1 \;\; \mathbf{0}_{3\times 1}] \in \mathbb{R}^{3\times 4}$. Changing the order of the inputs as in $\tilde{\mathbf{u}} = [u_1 \;\; u_2 \;\; u_3 \;\; u_5 \;\; u_4]^\top$, the decoupling matrix becomes $\tilde{\mathbf{E}} = \begin{bmatrix} \tilde{\mathbf{E}}_1 & \mathbf{0}_{1\times 3} \\ \tilde{\mathbf{e}}_3 & e_{\eta_i} \end{bmatrix}$, where

$$\tilde{\mathbf{E}}_1 = \bar{\mathbf{W}} \begin{bmatrix} \tilde{\mathbf{U}}_1 & \mathbf{0}_{3\times 1} \\ \mathbf{0}_{1\times 3} & 1 \end{bmatrix}, \tilde{\mathbf{e}}_3 = \begin{bmatrix} 0 & \mathbf{e}_i^\top \mathbf{T}_\eta \mathbf{J}_R^{-1}\mathbf{e}_1 & \mathbf{e}_i^\top \mathbf{T}_\eta \mathbf{J}_R^{-1}\mathbf{e}_2 & 0 \end{bmatrix},$$

$$\tilde{\mathbf{U}}_1 = -\mathbf{R}_C^\top \mathbf{R}_R \left[\mathbf{e}_3 - \frac{u_1}{J_{R11}}\mathbf{e}_2 \;\; \frac{u_1}{J_{R22}}\mathbf{e}_1\right] = -\mathbf{R}_C^\top \mathbf{R}_R \tilde{\mathbf{T}}.$$

The original decoupling matrix $\bar{\mathbf{E}}$ is invertible if $\tilde{\mathbf{E}}$ is invertible, or equivalently, due to its canonical form, if $\tilde{\mathbf{E}}_1$ is invertible and e_{η_i} is nonzero. Since the matrices $\mathbf{R}_C$, $\mathbf{R}_R$ and $\bar{\mathbf{W}}$ are always full rank (except in the model singularities, i.e., $l = 0$ and $\delta = \pm\pi/2$), then $\tilde{\mathbf{U}}_1$ is invertible whenever $\tilde{\mathbf{T}}$ is full rank, i.e., if $u_1 \neq 0$, indeed $\det(\tilde{\mathbf{T}}) = u_1^2/(J_{R11}J_{R22})$.

In the cases in which the thrust u_1 is not zero and with the opportune parametrization of $\mathbf{R}_R$, using the control law

$$\bar{\mathbf{u}} = \bar{\mathbf{E}}(\bar{\mathbf{x}}, \mathbf{X}_C^0)^{-1}\left[-\bar{\mathbf{b}}(\bar{\mathbf{x}}, \mathbf{X}_C^4) + \mathbf{v}^a\right], \tag{4.54}$$

where $\mathbf{v}^a = [v_1^a \;\; v_2^a \;\; v_3^a \;\; v_4^a \;\; v_5^a]^\top \in \mathbb{R}^5$ are virtual inputs, we obtain

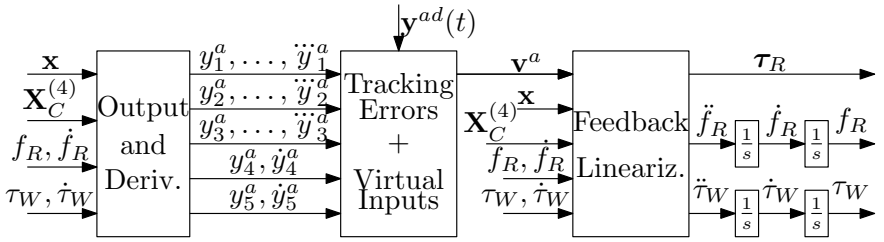

Fig. 4.4 Block diagram representation of the control strategy. © 2020 IEEE. Reprinted, with permission, from [10]

$$y_1^{a(4)} = v_1^a, \quad y_2^{a(4)} = v_2^a, \quad y_3^{a(4)} = v_3^a, \quad y_4^{a(2)} = v_4^a, \quad y_5^{a(2)} = v_5^a. \tag{4.55}$$

Furthermore, the total relative degree with respect to $\mathbf{y}^a$ is $r^a = 16$ that corresponds to the dimension of the extended state $\bar{\mathbf{x}}$ that is $\bar{n} = 16$. Indeed it is composed by $\mathbf{x}$ (of dimension 12) plus the four states of the dynamic compensator. Therefore the system is exactly dynamic feedback linearizable and the linearized system (4.55) does not have an internal dynamics [24].

4.6.1.1 Outer Linear Controller

In the following we will omit the subscript $\bullet^a$ since the same outer-loop control can be applied to track both $\mathbf{y}^a$ and $\mathbf{y}^b$, after the application of the opportune linearizing control law.

The tracking of any given desired trajectory, $y_i^d(t) \in C^3$ for $i = 1, 2, 3$ and $y_j^d(t) \in C^1$ for $j = 4, 5$ can be achieved applying any linear control technique to the equivalent linear system (4.55), as depicted in Fig. 4.4. As explained in Sect. 2.3, it is sufficient to use as outer loop a simple controller based on the pole placing technique. Setting the virtual control inputs as

$$v_i = y_i^{d(4)} + \mathbf{k}_i^\top \boldsymbol{\xi}_i, \qquad v_j = y_j^{d(2)} + \mathbf{k}_j^\top \boldsymbol{\xi}_j, \tag{4.56}$$

where $\boldsymbol{\xi}_i = [\xi_i^{(3)} \;\; \ddot{\xi}_i \;\; \dot{\xi}_i \;\; \xi_i]^\top \in \mathbb{R}^4, \boldsymbol{\xi}_j = [\dot{\xi}_j \;\; \xi_j]^\top \in \mathbb{R}^2, \xi_i = y_i^d - y_i$ and $\xi_j = y_j^d - y_j$ are the tracking errors, one can set the poles of the error dynamics through the gains $\mathbf{k}_i \in \mathbb{R}^4_{>0}$ and $\mathbf{k}_j \in \mathbb{R}^2_{>0}$, for $i = 1, 2, 3$ and $j = 4, 5$, to obtain a sufficiently fast exponentially tracking of the desired trajectories.

All the previous results are summarized in the following

Proposition *For the analyzed system it exists at least one parametrization $\boldsymbol{\eta}$ of $\mathbf{R}_R$ and one of its elements η_i such that $\mathbf{y}^a = [l \;\; \varphi \;\; \delta \;\; f_L \;\; \eta_i]^\top$ is an exact feedback linearizing output for each state, except if $l = 0$, $\delta = \pm\pi/2$ and $u_1 = 0$ (zero thrust case). Furthermore, considering as input $\bar{\mathbf{u}} = [\ddot{u}_1 \;\; u_2 \;\; u_3 \;\; u_4 \;\; \ddot{u}_5]^\top$, the control law*

$\bar{\mathbf{u}} = \Gamma^a_{DFL}(\bar{\mathbf{x}}, \mathbf{X}^4_C, \mathbf{y}^{ad}(t))$ *defined by (4.54) and (4.56) exponentially steers* $\mathbf{y}^a$ *along the desired trajectories* $y_i^{ad}(t) \in C^3$ *for* i=1, 2, 3, *and* $y_j^{ad}(t) \in C^1$ *for* j=4, 5. □

Remark In order to implement the exact tracking control laws (4.54)–(4.56) the only needed quantities are

- the desired output trajectory and its derivatives $y_i^{\star d}$, $\dot{y}_i^{\star d}$, $\ddot{y}_i^{\star d}$, $\dddot{y}_i^{\star d}$, $\ddddot{y}_i^{\star d}$ for $i = 1, 2, 3$, and $y_j^{\star d}$, $\dot{y}_j^{\star d}$, $\ddot{y}_j^{d}$ for $j = 4, 5$, where $y_i^\star$ is either y_i^a or y_i^b
- a measurement of system state, i.e., $\mathbf{x} = (\mathbf{q}, \dot{\mathbf{q}}, \mathbf{R}_R, \boldsymbol{\omega}_R)$
- the internal state of the compensators f_R, $\dot{f}_R$, $\bar{\tau}_W$, $\dot{\bar{\tau}}_W$
- the position and orientation of the moving platform and their derivatives $\mathbf{X}^4_C$. □

We recall that an explicit measurement of the output and its derivatives is not needed at all, since they are algebraic functions of the state and input.

4.6.2 Attitude-Related Feedback Linearizing Output

Now we are ready to show that $\mathbf{y}^b = [y_1^b \;\; y_2^b \;\; y_3^b \;\; y_4^b \;\; y_5^b]^\top = [l \;\; \varphi \;\; \delta \;\; \vartheta_A \;\; \eta_i]^\top \in \mathbb{R}^5$ is a feedback linearizing output. Similarly to Sect. 4.4.2, we firstly show that $\mathbf{y}^b$ and its derivatives can be written as a function of $\mathbf{y}^a$ and its derivatives, and $\mathbf{X}^i_C$ with $i > 0$. In particular, we shall show that $[\mathbf{y}_1^{b(4)} \;\; \ddot{y}_4^b \;\; \ddot{y}_5^b]^\top$, linearly depends on $[\mathbf{y}_1^{a(4)} \;\; \ddot{y}_4^a \;\; \ddot{y}_5^a]^\top$, i.e., there exists the functions $\mathbf{b}_{\mathbf{y}^b}(\mathbf{y}_1^a, \ldots, \mathbf{y}_1^{a(3)}, \mathbf{X}^4_C)$ and $\mathbf{E}_{\mathbf{y}^b}(\mathbf{y}_1^a, \mathbf{X}^0_C)$ such that

$$\begin{bmatrix} \mathbf{y}_1^{b(4)} \\ \ddot{y}_4^b \\ \ddot{y}_5^b \end{bmatrix} = \mathbf{b}_{\mathbf{y}^b}(\mathbf{y}_1^a, \ldots, \mathbf{y}_1^{a(3)}, \mathbf{X}^4_C) + \mathbf{E}_{\mathbf{y}^b}(\mathbf{y}_1^a, \mathbf{X}^0_C) \begin{bmatrix} \mathbf{y}_1^{a(4)} \\ \ddot{y}_4^a \\ \ddot{y}_5^a \end{bmatrix}. \tag{4.57}$$

Let us first extract $\mathbf{f}_R$ from (4.9), and differentiate it twice, showing the dependence on $\mathbf{y}^a$ and its derivatives:

$$\mathbf{f}_R = \underbrace{-\mathbf{R}_C(\mathbf{a}_x + \mathbf{a}_g)}_{\mathbf{b}'_{\mathbf{f}_R}(\mathbf{y}_1^a, \dot{\mathbf{y}}_1^a, \mathbf{X}^2_C)} + \underbrace{\left[m_R \mathbf{R}_C \mathbf{J}_\mathbf{q} \;\; \mathbf{d}\right]}_{\mathbf{E}_{\mathbf{f}_R}(\mathbf{y}_1^a, \mathbf{X}^0_C) = [\mathbf{E}'_{\mathbf{f}_R} \; \mathbf{e}''_{f_R}]} \bar{\mathbf{y}}^a \tag{4.58}$$

$$\ddot{\mathbf{f}}_R = \mathbf{b}_{\mathbf{f}_R}(\mathbf{y}_1^a, \ldots, \mathbf{y}_1^{a(3)}, \mathbf{X}^4_C) + \mathbf{E}_{\mathbf{f}_R}(\mathbf{y}_1^a, \mathbf{X}^0_C)\ddot{\bar{\mathbf{y}}}^a, \tag{4.59}$$

where $\mathbf{b}_{\mathbf{f}_R}$ gathers all the terms that do not depend on $\ddot{\bar{\mathbf{y}}}^a$. Similarly, can write $\mathbf{z}_R$ and its derivatives as function of $\mathbf{f}_R$ and its derivatives, and thus as function of $\mathbf{y}^a$ and its derivatives:

$$\mathbf{z}_R = \mathbf{f}_R / \|\mathbf{f}_R\| \tag{4.60}$$

$$\dot{\mathbf{z}}_R = 1/\|\mathbf{f}_R\| \, (\mathbf{I}_3 - \mathbf{z}_R \mathbf{z}_R^\top)\dot{\mathbf{f}}_R = \mathbf{E}_{\mathbf{z}_R}(\mathbf{y}_1^a, \dot{\mathbf{y}}_1^a, \mathbf{X}^2_C)\dot{\mathbf{f}}_R \tag{4.61}$$

$$\ddot{\mathbf{z}}_R = \mathbf{b}_{\mathbf{z}_R}(\mathbf{y}_1^a, \ldots, \mathbf{y}_1^{a(3)}, \mathbf{X}^4_C) + \mathbf{E}_{\mathbf{z}_R}\mathbf{E}_{\mathbf{f}_R}\ddot{\bar{\mathbf{y}}}^a, \tag{4.62}$$

where $\mathbf{b}_{\mathbf{z}_R}$ gathers all the terms that do not depend on $\ddot{\mathbf{y}}^a$.

Let us now compute the second derivative of $\boldsymbol{\alpha}$, expressing it as function of $\mathbf{y}^a$ and its derivatives, replacing the previous equations where necessary.

$$\ddot{\boldsymbol{\alpha}} = \mathbf{b}_{\boldsymbol{\alpha}}(\mathbf{y}_1^a, \ldots, \mathbf{y}_1^{a\,(3)}, \mathbf{X}_C^4) - \mathbf{P}_L \mathbf{E}_{\mathbf{z}_R} \mathbf{E}_{\mathbf{f}_R} \ddot{\mathbf{y}}^a, \tag{4.63}$$

where $\mathbf{b}_{\boldsymbol{\alpha}}$ gathers all the terms that do not depend on $\ddot{\mathbf{y}}^a$.

Finally, we can compute the derivatives of $y_4^b = \vartheta_A$ in order to obtain the form in (4.57)

$$\dot{y}_4^b = \frac{1}{\alpha_1^2 + \alpha_3^2} \begin{bmatrix} -\alpha_3 & \alpha_1 \end{bmatrix} \begin{bmatrix} \dot{\alpha}_1 \\ \dot{\alpha}_3 \end{bmatrix} = \underbrace{\frac{1}{\|\boldsymbol{\alpha}\|^2} \boldsymbol{\alpha}^\top \begin{bmatrix} -\mathbf{e}_3 & \mathbf{0} & \mathbf{e}_1 \end{bmatrix}}_{\mathbf{e}_{y_4^b}(\mathbf{y}_1^a, \ldots, \mathbf{y}_1^{a\,(3)}, \mathbf{X}_C^4)} \dot{\boldsymbol{\alpha}} \tag{4.64}$$

$$\ddot{y}_4^b = \mathbf{b}'_{y_4^b} - \mathbf{e}_{y_4^b} \ddot{\boldsymbol{\alpha}} = \mathbf{b}_{y_4^b} - \mathbf{e}_{y_4^b} \mathbf{P}_L \mathbf{E}_{\mathbf{z}_R} \mathbf{E}_{\mathbf{f}_R} \ddot{\mathbf{y}}^a \tag{4.65}$$

where $\mathbf{b}'_{y_4^b}$ and $\mathbf{b}_{y_4^b}$ gather all the terms that do not depend on $\ddot{\boldsymbol{\alpha}}$ and $\ddot{\mathbf{y}}^a$, respectively.

Finally, noticing that $\mathbf{y}_1^b = \mathbf{y}_1^a$ and $y_5^b = y_5^a$ we can write the following equation, equal to the sought form (4.57)

$$\begin{bmatrix} \mathbf{y}_1^{b\,(4)} \\ \ddot{y}_4^b \\ \ddot{y}_5^b \end{bmatrix} = \underbrace{\begin{bmatrix} \mathbf{0} \\ \mathbf{b}_{y_4^b} \\ 0 \end{bmatrix}}_{\mathbf{b}_{\mathbf{y}^b}(\mathbf{y}_1^a, \ldots, \mathbf{y}_1^{a\,(3)}, \mathbf{X}_C^4)} + \underbrace{\begin{bmatrix} \mathbf{I}_3 & 0 & 0 \\ \mathbf{e}'_{y_4^b} & \mathbf{e}''_{y_4^b} & 0 \\ \mathbf{0} & 0 & 1 \end{bmatrix}}_{\mathbf{E}_{\mathbf{y}^b}(\mathbf{y}_1^a, \mathbf{X}_C^0)} \begin{bmatrix} \mathbf{y}_1^{a\,(4)} \\ \ddot{y}_4^a \\ \ddot{y}_5^a \end{bmatrix}, \tag{4.66}$$

where $\mathbf{e}'_{y_4^b} = -\mathbf{e}_{y_4^b} \mathbf{P}_L \mathbf{E}_{\mathbf{z}_R} \mathbf{E}'_{\mathbf{f}_R}$ and $\mathbf{e}''_{y_4^b} = -\mathbf{e}_{y_4^b} \mathbf{P}_L \mathbf{E}_{\mathbf{z}_R} \mathbf{e}''_{\mathbf{f}_R}$. Now we are ready to prove that the system is dynamic feedback linearizable with respect to $\mathbf{y}^b$. From Sect. 4.6.1, notice that $(\mathbf{y}_1^a, \dot{\mathbf{y}}_1^a, \ddot{\mathbf{y}}_1^a, \mathbf{y}_1^{a\,(3)})$ is a function of $(\bar{\mathbf{x}}, \mathbf{X}_C^4)$. Furthermore, replacing (4.53) into (4.66) we obtain:

$$\begin{bmatrix} \mathbf{y}_1^{b\,(4)} \\ \ddot{y}_4^b \\ \ddot{y}_5^b \end{bmatrix} = \mathbf{b}_{\mathbf{y}^b} + \mathbf{E}_{\mathbf{y}^b} \bar{\mathbf{b}} + \mathbf{E}_{\mathbf{y}^b} \bar{\mathbf{E}} \bar{\mathbf{u}} = \bar{\mathbf{b}}_{\mathbf{y}^b}(\bar{\mathbf{x}}, \mathbf{X}_C^2) + \bar{\mathbf{E}}_{\mathbf{y}^b}(\bar{\mathbf{x}}, \mathbf{X}_C^0) \bar{\mathbf{u}}. \tag{4.67}$$

Therefore, we can conclude that $\mathbf{y}^b$ is a dynamic feedback linearizing output for all $\bar{\mathbf{x}}$ such that the decoupling matrix $\bar{\mathbf{E}}_{\mathbf{y}^b}$ is invertible, i.e., such that $\mathbf{E}_{\mathbf{y}^b}$ and $\bar{\mathbf{E}}$ are full rank. From Sect. 4.6.1, $\bar{\mathbf{E}}$ is full rank if $l \neq 0$, $\delta \neq \pm\pi/2$ and $u_1 \neq 0$. On the other hand, $\mathbf{E}_{\mathbf{y}^b}$ is invertible if $\mathbf{e}''_{y_4^b} \neq 0$. Recalling the expression of $\mathbf{e}''_{y_4^b}$, $\mathbf{E}_{\mathbf{y}^b}$ is invertible if

$$(\mathbf{P}_L \mathbf{z}_R)^\top \begin{bmatrix} -\mathbf{e}_3 & \mathbf{0} & \mathbf{e}_1 \end{bmatrix} \mathbf{P}_L (\mathbf{I}_3 - \mathbf{z}_R \mathbf{z}_R^\top) \mathbf{d} \neq 0. \tag{4.68}$$

In order to simplify the notation, let us define $\mathbf{v}_1 = \mathbf{P}_L \mathbf{z}_R$ and $\mathbf{v}_2 = \mathbf{P}_L(\mathbf{I}_3 - \mathbf{z}_R\mathbf{z}_R^\top)\mathbf{d}$. Noticing that $[-\mathbf{e}_3 \;\; \mathbf{0} \;\; \mathbf{e}_1]$ is the skew symmetric matrix relative to $\mathbf{e}_2$, we have that the previous inequality is equal to $\mathbf{v}_1^\top(\mathbf{e}_2 \times \mathbf{v}_2) \neq 0$, that we can also write as $\mathbf{e}_2^\top(\mathbf{v}_2 \times \mathbf{v}_1) \neq 0$. Since $\mathbf{v}_1$ and $\mathbf{v}_2$ belong to the same plane $\mathcal{P}_L$, $(\mathbf{v}_2 \times \mathbf{v}_1)$ is orthogonal to $\mathcal{P}_L$ and thus parallel to $\mathbf{y}_L$. Notice that $\mathbf{y}_L$ is equal to $\mathbf{e}_2$ in frame $\mathcal{F}_L$. Therefore $\mathbf{e}_2^\top(\mathbf{v}_2 \times \mathbf{v}_1) \neq 0$ if and only if $(\mathbf{v}_2 \times \mathbf{v}_1) \neq \mathbf{0}$.

In order to study the conditions for which $\mathbf{P}_L(\mathbf{I}_3 - \mathbf{z}_R\mathbf{z}_R^\top)\mathbf{d} \times \mathbf{P}_L\mathbf{z}_R \neq 0$, we can show that $\mathbf{P}_L(\mathbf{I}_3 - \mathbf{z}_R\mathbf{z}_R^\top)\mathbf{d} \times \mathbf{P}_L\mathbf{z}_R = \mathbf{P}_L\mathbf{d} \times \mathbf{P}_L\mathbf{z}_R$. Indeed,

$$\mathbf{P}_L(\mathbf{I}_3 - \mathbf{z}_R\mathbf{z}_R^\top)\mathbf{d} \times \mathbf{P}_L\mathbf{z}_R - \mathbf{P}_L\mathbf{d} \times \mathbf{P}_L\mathbf{z}_R = \mathbf{0} \tag{4.69a}$$

$$\left(\mathbf{P}_L(\mathbf{I}_3 - \mathbf{z}_R\mathbf{z}_R^\top)\mathbf{d} - \mathbf{P}_L\mathbf{d}\right) \times \mathbf{P}_L\mathbf{z}_R = \mathbf{0} \tag{4.69b}$$

$$\mathbf{P}_L\mathbf{z}_R\mathbf{z}_R^\top\mathbf{d} \times \mathbf{P}_L\mathbf{z}_R = \mathbf{0}. \tag{4.69c}$$

The previous equivalent conditions always hold since $\mathbf{z}_R\mathbf{z}_R^\top$ is the projector on $\mathbf{z}_R$ and therefore $\mathbf{z}_R\mathbf{z}_R^\top\mathbf{d}$ is always parallel to $\mathbf{P}_L\mathbf{z}_R$ (or zero).

Finally, we have that $\mathbf{E}_{\mathbf{y}^b}$ is invertible if $\mathbf{P}_L\mathbf{d} \times \mathbf{P}_L\mathbf{z}_R \neq \mathbf{0}$, and therefore if $\mathbf{z}_R$ is not perpendicular to the plane $\mathcal{P}_L$ and if $\mathbf{P}_L\mathbf{z}_R$ and $\mathbf{P}_L\mathbf{d}$ are not parallel, i.e., if $\mathbf{z}_R \not\perp \mathcal{P}_L$ and $\mathbf{P}_L\mathbf{z}_R \nparallel \mathbf{P}_L\mathbf{d}$. Summarizing, the decoupling matrix $\bar{\mathbf{E}}_{\mathbf{y}^b}$ is invertible, and thus $\mathbf{y}^b$ is a feedback linearizing output, for all the states except if $l = 0$ and $\delta = \pm\pi/2$ (singularity of the spherical coordinates), $u_1 = 0$ (singularity of the feedback linearization with respect to $\mathbf{y}^a$), $\mathbf{z}_R \perp \mathcal{P}_L$ and $\mathbf{P}_L\mathbf{z}_R \parallel \mathbf{P}_L\mathbf{d}$.

In the cases in which $\bar{\mathbf{E}}_{\mathbf{y}^b}$ is invertible, using the control law

$$\bar{\mathbf{u}} = \bar{\mathbf{E}}_{\mathbf{y}^b}(\bar{\mathbf{x}}, \mathbf{X}_C^0)^{-1}\left[-\bar{\mathbf{b}}_{\mathbf{y}^b}(\bar{\mathbf{x}}, \mathbf{X}_C^2) + \mathbf{v}^b\right], \tag{4.70}$$

where $\mathbf{v}^b = [v_1^b \;\; v_2^b \;\; v_3^b \;\; v_4^b \;\; v_5^b]^\top \in \mathbb{R}^5$ are virtual inputs, we obtain

$$y_1^{b(4)} = v_1^b, \quad y_2^{b(4)} = v_2^b, \quad y_3^{b(4)} = v_3^b, \quad y_4^{b(2)} = v_4^b, \quad y_5^{b(2)} = v_5^b. \tag{4.71}$$

Furthermore, the total relative degree with respect to $\mathbf{y}^b$ is $r^b = 16$ that corresponds to the dimension of the extended state $\bar{\mathbf{x}}$ that is $\bar{n} = 16$. Therefore the system is exactly dynamic feedback linearizable and the linearized system (4.71) does not have an internal dynamics.

As done in Sect. 4.6.1, to track a desired trajectory $\mathbf{y}^{bd}(t)$, we can apply to the linearized system (4.71) a linear controller, as the one in (4.56) obtaining a control strategy similar to the one represented in Fig. 4.4.

Proposition *For the analyzed system it exists at least one parametrization $\boldsymbol{\eta}$ of $\mathbf{R}_R$ and one of its elements η_i such that $\mathbf{y}^b = [l \;\; \varphi \;\; \delta \;\; \vartheta_A \;\; \eta_i]^\top$ is an exact feedback linearizing output for each state, except if $l = 0$, $\delta = \pm\pi/2$, $u_1 = 0$, $\mathbf{z}_R \perp \mathcal{P}_L$ and $\mathbf{P}_L\mathbf{z}_R \parallel \mathbf{P}_L\mathbf{d}$. Furthermore, considering as input $\bar{\mathbf{u}} = [\ddot{u}_1 \;\; u_2 \;\; u_3 \;\; u_4 \;\; \ddot{u}_5]^\top$, the control law $\bar{\mathbf{u}} = \Gamma_{DFL}^b(\bar{\mathbf{x}}, \mathbf{X}_C^4, \mathbf{y}^{bd}(t))$ defined by (4.70) and (4.56) (properly adapted), exponentially steers $\mathbf{y}^b$ along the desired trajectories $y_i^{bd}(t) \in C^3$ for $i = 1, 2, 3$, and $y_j^{bd}(t) \in C^1$ for $j = 4, 5$.* □

4.6.3 Dynamic Feedback Linearization for Passive Link Actuator

Considering $\mathbf{y}^c$ as output of interest and applying the feedback linearization technique, we need to differentiate each entry of $\mathbf{y}^c$ until the input appears. From (4.16) and (4.44), $\mathbf{y}^c$ has to be differentiated twice to see the input appear:

$$\begin{bmatrix} \ddot{\mathbf{y}}_1^c \\ \ddot{y}_4^c \end{bmatrix} = \begin{bmatrix} \bar{\mathbf{M}}\mathbf{a} \\ b_{\eta_i} \end{bmatrix} + \begin{bmatrix} \bar{\mathbf{M}}\mathbf{Q} \\ \mathbf{e}_{\eta_i} \end{bmatrix} \mathbf{u} = \underbrace{\begin{bmatrix} \bar{\mathbf{M}}\mathbf{a}' \\ b_{\eta_i} \end{bmatrix}}_{\mathbf{b}_{\mathbf{y}^c}(\mathbf{x}, \mathbf{X}_C^2)} + \underbrace{\begin{bmatrix} -\mathbf{J}_\mathbf{q}^\top \mathbf{R}_C^\top \mathbf{R}_R \mathbf{e}_3 & \mathbf{0}_{3\times 3} \\ 0 & \mathbf{e}_i^\top \mathbf{T}_{\boldsymbol{\eta}} \mathbf{J}_R^{-1} \end{bmatrix}}_{\mathbf{E}_{\mathbf{y}^c}(\mathbf{x}, \mathbf{X}_C^0)} \mathbf{u}', \tag{4.72}$$

where $\bar{\mathbf{M}} = \mathbf{M}'^{-1}$ and $\mathbf{a}' = -\mathbf{c}' - \mathbf{g}' - \mathbf{n}' - \mathbf{w}'$. Similarly to the previous cases, the decoupling matrix $\mathbf{E}_{\mathbf{y}^c}$ is singular for every conditions because $\boldsymbol{\tau}_R$ does not appear on $\ddot{\mathbf{y}}_1^c$. This means that the system is not statically feedback linearizable.

As done before, we can apply a dynamic feedback inserting a dynamic compensator in the control u_1. Consider as new input the second derivative of the thrust and the torque, i.e., $\bar{\mathbf{u}}' = [\ddot{u}_1 \;\; \mathbf{u}_2^\top]^\top$. Now $\ddot{\mathbf{y}}_1^c$ has to be differentiated four times to see $\bar{\mathbf{u}}'$ appear, while for y_4^c everything remains the same, indeed:

$$\begin{bmatrix} \ddot{\mathbf{y}}_1^{c\,(4)} \\ y_4^c \end{bmatrix} = \begin{bmatrix} \ddot{\bar{\mathbf{M}}}(\mathbf{a}' + \mathbf{a}_{\mathbf{u}'}) + 2\dot{\bar{\mathbf{M}}}(\dot{\mathbf{a}}' + \dot{\mathbf{a}}_{\mathbf{u}'}) + \bar{\mathbf{M}}(\ddot{\mathbf{a}}' + \ddot{\mathbf{a}}_{\mathbf{u}'}) \\ b_i + \mathbf{e}_{\eta_i} \bar{\mathbf{u}} \end{bmatrix}, \tag{4.73}$$

where $\ddot{\mathbf{a}}_{\mathbf{u}'}$, after replacing the system dynamics, results:

$$\ddot{\mathbf{a}}_{\mathbf{u}'} = \bar{\ddot{\mathbf{a}}}_{\mathbf{u}'} + \mathbf{J}_\mathbf{q}^\top \mathbf{R}_C^\top \mathbf{R}_R (-\ddot{u}_1 \mathbf{e}_3 - u_1 \left[\mathbf{J}_R^{-1} \boldsymbol{\tau}_R\right]_\times \mathbf{e}_3), \tag{4.74}$$

where $\bar{\ddot{\mathbf{a}}}_{\mathbf{u}'}$ gathers all the terms that do not depend on $\bar{\mathbf{u}}'$. Replacing Eqs. (4.52) and (4.74) into (4.73) we obtain

$$\begin{bmatrix} \mathbf{y}_\mathbf{q}^{(4)} \\ \ddot{y}_4 \end{bmatrix} = \bar{\mathbf{b}}_{\mathbf{y}^c}(\bar{\mathbf{x}}, \mathbf{X}_C^4) + \underbrace{\begin{bmatrix} \bar{\mathbf{M}}\mathbf{J}_\mathbf{q}^\top \mathbf{R}_C^\top \mathbf{R}_R \mathbf{T} \; \mathbf{0}_{3\times 1} \\ \tilde{\mathbf{e}}_3 \qquad \tilde{e}_2 \end{bmatrix}}_{\bar{\mathbf{E}}_{\mathbf{y}^c}(\bar{\mathbf{x}}, \mathbf{X}_C^0)} \bar{\mathbf{u}}', \tag{4.75}$$

where $\bar{\mathbf{b}}(\bar{\mathbf{x}}, \mathbf{X}_C^4)$ collects all the terms that do not depend on $\bar{\mathbf{u}}'$, $\tilde{e}_2 = \mathbf{e}_i^\top \mathbf{T}_{\boldsymbol{\eta}} \mathbf{J}_R^{-1} \mathbf{e}_3$, and $\tilde{\mathbf{e}}_3 = \mathbf{e}_i^\top \mathbf{T}_{\boldsymbol{\eta}} \mathbf{J}_R^{-1} [\mathbf{0}_{3\times 1} \;\; \mathbf{e}_1 \;\; \mathbf{e}_2]$. Similar to Sect. 4.6.1, the decoupling matrix $\bar{\mathbf{E}}_{\mathbf{y}^c}$ results to be invertible if $u_1 \neq 0$ and if the parametrization $\boldsymbol{\eta}$ of $\mathbf{R}_R$ and one of its elements η_i are chosen such that $\tilde{e}_2 \neq 0$, i.e., if (4.45) is verified in the domain of interest. Then, in the case in which $\bar{\mathbf{E}}_{\mathbf{y}^c}$ is invertible, defining $\mathbf{v}^c = [v_1^c \;\; v_2^c \;\; v_3^c \;\; v_4^c]^\top \in \mathbb{R}^4$ as virtual inputs, the control law

$$\bar{\mathbf{u}}' = \bar{\mathbf{E}}_{\mathbf{y}^c}(\bar{\mathbf{x}}, \mathbf{X}_C^0)^{-1}\left[-\bar{\mathbf{b}}_{\mathbf{y}^c}(\bar{\mathbf{x}}, \mathbf{X}_C^4) + \mathbf{v}^c\right], \tag{4.76}$$

brings the original system in the equivalent linear one:

$$y_1^{c(4)} = v_1^c, \quad y_2^{c(4)} = v_2^c, \quad y_3^{c(4)} = v_3^c, \quad y_4^{c(2)} = v_4^c. \tag{4.77}$$

This means that the system results to be exactly linearizable through dynamic feedback and the linearized system (4.77) does not have an internal dynamics. Indeed, the total relative degree with respect to $\mathbf{y}^c$ is $r^c = 4 + 4 + 4 + 2 = 14 = \bar{n}$, where $\bar{n}$ is dimension of the extended state $\bar{\mathbf{x}}$.

As done in Sect. 4.6.1, to track a desired trajectory $\mathbf{y}^{cd}(t)$, we can apply to the linearized system (4.77) a linear controller as the one in (4.56) obtaining a control strategy similar to the one represented in Fig. 4.4.

Proposition *For the analyzed system it exists at least one parametrization $\boldsymbol{\eta}$ of $\mathbf{R}_R$ and one of its elements η_i such that $\mathbf{y}^c = [l \ \varphi \ \delta \ \eta_i]^\top$ is an exact feedback linearizing output for each state, except if $l = 0$, $\delta = \pm\pi/2$, $u_1 = 0$. Furthermore, considering as input $\bar{\mathbf{u}}' = [\ddot{u}_1 \ u_2 \ u_3 \ u_4]^\top$, the control law $\bar{\mathbf{u}}' = \Gamma^c_{DFL}(\bar{\mathbf{x}}, \mathbf{X}_C^4, \mathbf{y}^{cd}(t))$ defined by (4.76) and (4.56) (properly adapted), exponentially steers $\mathbf{y}^c$ along the desired trajectories $y_i^{cd}(t) \in C^3$ for $i = 1, 2, 3$, and $y_4^{cd}(t) \in C^1$.* □

4.6.4 Dynamic Feedback Linearization for the Reduced Model

It is easy to recast all the controllers presented so far for the reduced model presented in Sect. 4.3. Indeed this is a sub-case of the general system. However, we found out that for this reduced morel, the tracking of the output $\mathbf{y}_r^b = [\varphi \ \vartheta_A]^\top$ can be obtained with a simpler static-feedback linearizing controller, $\Gamma^b_{\text{SFL}r}$. For the corresponding details we refer the interested reader to[6] [12]. Notice that the control actions required by this controller may be discontinuous due to, e.g., desired trajectories possessing a discontinuity in the second derivative or simply, in the real case, due to some noise in the measurements. This has to be taken into account in case one would like, e.g., to minimize mechanical vibrations of the link. Furthermore, as recalled in Sect. 3.3.1, one has to keep in mind that discontinuous inputs cannot be performed by the physical system in exam because the acceleration of both propeller rotation and the corresponding air flow cannot be infinite. However, if one needs to enforce smoother inputs it possible to apply a dynamic compensator in order to get a sufficiently smooth control signal.

Table 4.4 summarizes all the controllers designed so far for the general and particular systems.

[6] Notice that in [12] we considered θ as part of the output instead of ϑ_A. However, in the 2D plane, $\vartheta_A = \theta$ so the results are still valid.

Table 4.4 List of designed controllers with the corresponding main features and characteristics

Ctrl.	Cont. outputs	Goal	Method	Type	Singularities
Γ^a_{HC}	$(l, \varphi, \delta, f_L, \eta_i)$	Stabilization	Hierarchical	Static	$f_R = 0$
Γ^b_{HC}	$(l, \varphi, \delta, \vartheta_A, \eta_i)$	Stabilization	Hierarchical	Static	$f_R = 0$, $\mathbf{z}_R \perp \mathcal{P}_L$, $\mathbf{P}_L\mathbf{z}_R \parallel \mathbf{P}_L\mathbf{d}$
Γ^c_{HC}	$(l, \varphi, \delta, \eta_i)$	Stabilization (passive link actuator)	Hierarchical	Static	$f_R = 0$
Γ^a_{DFL}	$(l, \varphi, \delta, f_L, \eta_i)$	Tracking	DFL	Dynamic	$f_R = 0, l = 0$, $\delta = \pm\pi/2$
Γ^b_{DFL}	$(l, \varphi, \delta, \vartheta_A, \eta_i)$	Tracking	DFL	Dynamic	$f_R = 0, l = 0$, $\delta = \pm\pi/2$, $\mathbf{z}_R \perp \mathcal{P}_L$, $\mathbf{P}_L\mathbf{z}_R \parallel \mathbf{P}_L\mathbf{d}$
Γ^c_{DFL}	$(l, \varphi, \delta, \eta_i)$	Tracking (passive link actuator)	DFL	Dynamic	$f_R = 0, l = 0$, $\delta = \pm\pi/2$
$\Gamma^b_{\text{SFL}^r}$	(φ, ϑ_A)	Tracking (reduced model)	SFL	Static	$\vartheta_A = 0$

4.7 State Estimation

In Remark 4.6.1.1 we already highlighted the fact that in order to compute the control action, only the system state and the knowledge of the trajectory of the platform are needed. Assuming that $\mathbf{w}_1 = \mathbf{X}^4_C$ (we recall that $\mathbf{X}^4_C$ is defined in (4.13)) is a priori known or it is estimated/measured on-line by a set of sensors, then only the knowledge of $\mathbf{x}$ is need to close the control loop. One could directly measure $\mathbf{x}$ by using a collection of sensors such as a GPS, cameras, tracking systems etc. In this section we shall demonstrate that exploiting the tautness of the cable (i.e., when $f_L \neq 0$) it is possible to retrieve $\mathbf{x}$ from a standard set of sensors summarized in Table 4.5. In particular, from the moving platform side, we assume to have an encoder that measures the absolute rotation of the link actuator. Assuming no backlash and constant radius r_W, this is equivalent to measure the length of the link, i.e., $w_2 = r_W\vartheta_W = l$. Furthermore, using a gimbal-like system based on two encoders (see [4] for a similar mechanism), we can measure the direction of the link, i.e., $w_3 = \varphi$ and $w_4 = \delta$.

The aerial vehicle is instead equipped with a standard sensory configuration composed by a 3-axis accelerometer, gyroscope and magnetometer mounted on O_R and aligned along the axis of $\mathcal{F}_R$. Recalling the sensor models provided in Sect. 3.4, the accelerometer measures the specific acceleration of O_R in $\mathcal{F}_R$, i.e.:

$$\mathbf{w}_5 = \mathbf{R}_R^\top(\ddot{\mathbf{p}}_R^W + g\mathbf{e}_3). \tag{4.78}$$

The gyroscope measures the angular velocity of $\mathcal{F}_R$ with respect to $\mathcal{F}_W$, expressed in $\mathcal{F}_R$, i.e., $\mathbf{w}_6 = \boldsymbol{\omega}_R$. Finally the magnetometer measures the known unit vector $\mathbf{h}^W \in \mathsf{S}^2$ describing the magnetic field direction expressed in $\mathcal{F}_R$:

$$\mathbf{w}_7 = \mathbf{R}_R^\top \mathbf{h}^W. \tag{4.79}$$

Using this sensory configuration, part of the state is already measured, though it remains to estimate $\mathbf{R}_R$ and $\dot{\mathbf{q}}$. From the accelerometer, replacing (4.5) into (4.78), we obtain

$$f_L \mathbf{R}_R^\top \mathbf{R}_C(\mathbf{w}_1)\mathbf{d}^C(w_3, w_4) = -m_R \mathbf{w}_5 - f_R \mathbf{e}_3. \tag{4.80}$$

We define $w_8 = \|-m_R \mathbf{w}_5 - f_R \mathbf{e}_3\|$. Notice that, since the controller guarantees a taut/compressed link, it must be that $f_L \neq 0$, thus $w_8 = f_L$. Defining $\mathbf{s}_1^R = (-m_R \mathbf{w}_5 - f_R \mathbf{e}_3)/w_8$ and $\mathbf{s}_1^W = \mathbf{R}_C(\mathbf{w}_1)\mathbf{d}^C(w_3, w_4)$ we have that $\mathbf{R}_R \mathbf{s}_1^R = \mathbf{s}_1^W$. Using also the magnetometer we obtain a direct measurement of $\mathbf{R}_R$ in the following way. Under the assumption that $\mathbf{s}_1^R$ and $\mathbf{w}_7$ are not parallel, let us define $\mathbf{s}_2^R = (\mathbf{s}_1^R \times \mathbf{w}_7)/\left\|\mathbf{s}_1^R \times \mathbf{w}_7\right\|$ and $\mathbf{s}_3^R = \mathbf{s}_1^R \times \mathbf{s}_2^R$. We then get

$$\mathbf{R}_R \mathbf{s}_2^R = \mathbf{R}_R(\mathbf{s}_1^R \times \mathbf{w}_7) = \mathbf{s}_1^W \times \mathbf{h}^W = \mathbf{s}_2^W \tag{4.81}$$

$$\mathbf{R}_R \mathbf{s}_3^R = \mathbf{R}_R(\mathbf{s}_1^R \times \mathbf{s}_2^R) = \mathbf{s}_1^W \times \mathbf{s}_2^W = \mathbf{s}_3^W, \tag{4.82}$$

where $\{\mathbf{s}_1^R, \mathbf{s}_2^R, \mathbf{s}_3^R\}$ is an orthonormal basis and $\mathbf{S}^R = [\mathbf{s}_1^R \ \mathbf{s}_2^R \ \mathbf{s}_3^R] \in \mathsf{SO}(3)$. Then, defining $\mathbf{S}^W = [\mathbf{s}_1^W \ \mathbf{s}_2^W \ \mathbf{s}_3^W]$, we obtain a direct measurements of $\mathbf{R}_R$ from the sensors $(\mathbf{w}_1, w_3, w_4, \mathbf{w}_5, \mathbf{w}_7)$ as:

$$\mathbf{R}_R = \mathbf{S}^W {\mathbf{S}^R}^\top = \mathbf{W}_R(\mathbf{w}_1, w_3, w_4, \mathbf{w}_5, \mathbf{w}_7). \tag{4.83}$$

Notice that we can find $\mathbf{R}_R$ only if $\mathbf{d}^W$ and $\mathbf{h}^W$ are not parallel (otherwise $\mathbf{s}_1^W \times \mathbf{h}^W = \mathbf{0}_3$) and if $f_L \neq 0$. Indeed, if $f_L = 0$ the link becomes slack and the aerial vehicle results decoupled from the rest of the system. In this condition is then not

Table 4.5 List of sensors

#	Type	Position	Reference	Measurement
$\mathbf{w}_1$	–	O_C	$\mathcal{F}_W$	$\mathbf{X}_C^4$
w_2	Absolute encoder	O_C	$\mathcal{F}_C$	$\vartheta_W \approx l$
w_3	Absolute encoder	O_C	$\mathcal{F}_C$	φ
w_4	Absolute encoder	O_C	$\mathcal{F}_C$	δ
$\mathbf{w}_5$	Accelerometer	O_R	$\mathcal{F}_R$	$\mathbf{R}_R(\ddot{\mathbf{p}}_R^W - g\mathbf{e}_3)$
$\mathbf{w}_6$	Gyroscope	O_R	$\mathcal{F}_R$	$\boldsymbol{\omega}_R$
$\mathbf{w}_7$	Magnetometer	O_R	$\mathcal{F}_R$	$\mathbf{R}_R \mathbf{h}^W$

possible to estimate the attitude of the vehicle in a direct way. Nevertheless, this is not a practical issue since the proposed controller guarantees any non zero internal force.[7] Regarding the special case in which we ask a zero internal force for just an instant, e.g., passing from tension to compression, we provide a short discussion in Sect. 4.9. Furthermore, the magnetometer can be replaced with any sensor able to measure a known vector in $\mathcal{F}_W$ expressed in $\mathcal{F}_R$ not parallel to $\mathbf{d}^W$. In the presence of noisy measurements one can exploit $\mathbf{W}_R$ and $\mathbf{w}_6$ designing a filter to obtain a better estimation of $\mathbf{R}_R$ and $\boldsymbol{\omega}_R$ [26].

After having shown how to estimate $\mathbf{R}_R$ from the measurements, it remains to estimate $\dot{\mathbf{q}}$. Defining $\mathbf{z} = [l \;\; \dot{l} \;\; \varphi \;\; \dot{\varphi} \;\; \delta \;\; \dot{\delta}] \in \mathbb{R}^6$ we can write its dynamics (see (4.11)) and the respective measurements as

$$\begin{aligned} \dot{\mathbf{z}} &= \mathbf{A}\mathbf{z} + \mathbf{B}\boldsymbol{\sigma}(\mathbf{z}, \mathbf{u}_t, \mathbf{R}_R, \mathbf{X}_C^2) \\ \mathbf{w}_\mathbf{z} &= [w_2 \;\; w_3 \;\; w_4]^\top = \mathbf{C}\mathbf{z}, \end{aligned} \tag{4.84}$$

where[8] $\mathbf{A} = \text{diag}(\mathbf{A}', \mathbf{A}', \mathbf{A}')$, $\mathbf{B} = \text{diag}(\mathbf{B}', \mathbf{B}', \mathbf{B}')$, $\mathbf{C} = \text{diag}(\mathbf{C}', \mathbf{C}', \mathbf{C}')$, $\mathbf{A}' = \left[\begin{smallmatrix} 0 & 1 \\ 0 & 0 \end{smallmatrix}\right]$, $\mathbf{B}' = \left[\begin{smallmatrix} 0 \\ 1 \end{smallmatrix}\right]$, $\mathbf{C}' = [\,1\;0\,]$. Thanks to the particular canonical form of (4.84), in order to get an estimation of $\mathbf{z}$, it is possible to apply the following nonlinear *high gain observer* (HGO) (see Sect. 2.4)

$$\dot{\hat{\mathbf{z}}} = \mathbf{A}\hat{\mathbf{z}} + \mathbf{B}\boldsymbol{\sigma}(\hat{\mathbf{z}}, \mathbf{u}_t, \mathbf{W}_R, \mathbf{w}_1) + \mathbf{H}(\mathbf{w}_\mathbf{z} - \mathbf{C}\hat{\mathbf{z}}), \tag{4.85}$$

where $\mathbf{H} = \text{diag}(\mathbf{H}', \mathbf{H}', \mathbf{H}')$ and $\mathbf{H}' = [\frac{\alpha_1}{\epsilon} \;\; \frac{\alpha_2}{\epsilon^2}]^\top$, with $\epsilon \in \mathbb{R}_{>0}$, and the gains $(\alpha_1, \alpha_2) \in \mathbb{R}_{>0}$ are set such that the roots of $s^2 + \alpha_1 s + \alpha_2$ have negative real part. The gains (α_1, α_2) influence the convergence rate of the estimation.

Summarizing, using the standard sensory configuration of Table 4.5, we were able to achieve the third goal obtaining an estimation of the whole state:

$$\begin{aligned} \hat{l} = \hat{z}_1 \;\; \hat{\varphi} = \hat{z}_3 \;\; \hat{\delta} = \hat{z}_5 \;\; \hat{\mathbf{R}}_R = \mathbf{W}_R \\ \hat{\dot{l}} = \hat{z}_2 \;\; \hat{\dot{\varphi}} = \hat{z}_4 \;\; \hat{\dot{\delta}} = \hat{z}_6 \;\; \hat{\boldsymbol{\omega}}_R = \mathbf{w}_6. \end{aligned} \tag{4.86}$$

4.7.1 Closed Loop Stability

In Sect. 4.6 we saw that the control law Γ^a_{DFL}, Γ^b_{DFL} and Γ^c_{DFL} need only the knowledge of the state and of the trajectory of the platform in order to close the loop. Thus we can use the state estimation provided by the proposed observer as feedback for the controller. Though, since the system is nonlinear, one cannot apply the separation

[7] As already said, in a preliminary phase one can bring the cable in a taut condition using a near hovering control [25]. Then it can be replaced with our controller to maintain the desired tension or compression.

[8] $\text{diag}(\mathbf{X}_1, \ldots, \mathbf{X}_n)$ is a block matrix having on the main block diagonal the matrices $\mathbf{X}_i$, whereas the off-diagonal blocks are zero matrices.

principle like in the linear case. Nevertheless, thanks to the direct measurements of some entry of the state and to the particular kind of translational dynamics, i.e., triangular block dynamics with a direct measurement of the first state of each block, it can be shown that a strong property holds [24]. In fact, since the closed loop system by the state feedback controller is exponentially stable for every state except the its singularities (see Table 4.4), there exist a $\bar{\epsilon}$ such that, for every $0 < \epsilon \leq \bar{\epsilon}$ in (4.85), the closed loop system with the observer is exponentially stable, except for the zero stress case and for the controller singularities [24] (see Sect. 2.4).

4.7.2 Discussion on Platform State Measurement

To obtain a perfect tracking one has to know the derivatives of $\mathbf{p}_C^C(t)$ up to the fourth order and of $\boldsymbol{\omega}_C(t)$ up to the third order (see Sect. 4.6). Although any controller (not only the one proposed here) needs to know (implicitly or explicitly) those variables to obtain a zero tracking error, it is difficult in practice to directly measure the higher-order derivatives.

In order to overcome such issue, some practical techniques could be applied which are here shortly mentioned. If the model and control input of the system are known (e.g., in the case of an autonomous vehicle), an observer can be designed to retrieve the needed derivatives of $\mathbf{p}_C^C$ and $\boldsymbol{\omega}_C$. Without the dynamic model but with a set of measurements of some derivatives, one can use standard tracking technique or, if the trajectory of the vehicle is sufficiently 'low frequency', the missing higher derivatives could be simply assumed negligible and equal to zero. For the last case, in Sect. 5.3 we show that the tracking error remains small and bounded.

4.8 State Estimation for the Reduced Model

As said in the previous section, finding the minimal sensory setup that still allows to retrieve the full state estimation is a very important problem, for safety but also for technical and cost-related problems. Driven by these practical reasons and also by the intrinsic theoretical appeal of solving control problems with minimal sensing, in this section we show that the standard on-board inertial sensor (i.e., an accelerometer plus a gyroscope) is sufficient to estimate the full state of the reduced system presented at the end of Sect. 4.3. We recall that the latter consists of a tethered aerial vehicles constrained to move on a 2D vertical plane, with the link fixed to the ground and characterized by a constant length. Its dynamics is given by (4.18). We then show the design of an exact nonlinear observer for that purpose. Of course the state estimator designed in Sect. 4.7 can be still applied for the 2D case, but the corresponding sensory setup results non minimal. Indeed, the encoder directly measuring the elevation is not needed in this case.

Under the 2D constraints we can redefine the state vector as $\mathbf{x} = [\varphi \ \dot{\varphi} \ \theta \ \dot{\theta}]^\top = [x_1 \ x_2 \ x_3 \ x_4]^\top \in \mathbb{R}^4$ and the input vector as $\mathbf{u} = [f_R \ \tau_{Ry}]^\top = [u_1 \ u_2]^\top$. In view of those definitions we can rewrite the 2D dynamic model (4.18) in a more convenient state space form:

$$\dot{\mathbf{x}} = \begin{bmatrix} x_2 \\ a_1 c_{x_1} \\ x_4 \\ 0 \end{bmatrix} + \begin{bmatrix} 0 & 0 \\ a_2 c_{x_1+x_3} & 0 \\ 0 & 0 \\ 0 & a_3 \end{bmatrix} \mathbf{u}, \tag{4.87}$$

where $a_1 = -g/l$, $a_2 = 1/(m_R l)$, $a_3 = 1/J_{R22}$ are the constant parameters of the dynamical model. As normal in the literature we define $s_\star = \sin(\star)$ and $c_\star = \cos(\star)$. Again, the on-board inertial sensor provides the following measurements:

$$\omega = x_4 \tag{4.88}$$

$$\mathbf{a} = \mathbf{R}_R^\top (\ddot{\mathbf{p}}_R + g\mathbf{z}_W) = \begin{bmatrix} a_x & a_y & a_z \end{bmatrix}^\top. \tag{4.89}$$

From now on we omit the second row which is zero by construction, i.e., we assume $\mathbf{a} = \begin{bmatrix} a_x & a_z \end{bmatrix}^\top$.

Observing the full state of system (4.87) using the partial measurements (4.88), and (4.89) is a nontrivial nonlinear observation problem, where the nonlinearities appear both in the system dynamics and in the measurements. We show in the following how this problem can be successfully tackled. Fist of all exploiting (4.88) we can define the gyroscope measurement as a new input $u_3 = \omega$ that lets us reduce the system dimension from four to three. Then, substituting (4.7) and (4.87) into (4.89) and performing some simple algebraic manipulation on the accelerometer measurement we obtain

$$\begin{bmatrix} \dot{x}_1 \\ \dot{x}_2 \\ \dot{x}_3 \end{bmatrix} = \begin{bmatrix} 0 & 1 & 0 \\ 0 & 0 & 0 \\ 0 & 0 & 0 \end{bmatrix} \begin{bmatrix} x_1 \\ x_2 \\ x_3 \end{bmatrix} + \begin{bmatrix} 0 \\ a_1 c_{x_1} + a_2 c_{x_1+x_3} u_1 \\ u_3 \end{bmatrix} \tag{4.90}$$

$$\mathbf{a} = \begin{bmatrix} l c_{x_1+x_3} \left(x_2^2 + a_1 s_{x_1} + a_2 s_{x_1+x_3} u_1 \right) \\ l s_{x_1+x_3} \left(x_2^2 + a_1 s_{x_1} + a_2 s_{x_1+x_3} u_1 \right) - a_2 u_1 \end{bmatrix}. \tag{4.91}$$

The problem is then 'reduced' to the observation of the state $[x_1 \ x_2 \ x_3]^\top$ from the knowledge of the measurements $\mathbf{a}$ and the inputs $[u_1 \ u_3]^\top$. However this problem is still nonlinear both in the system dynamics and in the measurement map.

Trying to apply the exact nonlinear high gain observer also in this case, the system should be in the canonical form (2.15). Although at first view system (4.90 and 4.91) does not resemble to a system in canonical form, we shall demonstrate in the following that it can be put in that form using a few appropriate nonlinear transformations.

4.8.1 State/Output Transformations and HGO Design

In the following we prove that there exist a change of coordinates from the original state $\mathbf{x}$ to a new state $\mathbf{z} = [z_1\ z_2\ z_3]^\top$ and from the original measurements $\mathbf{a}$ to a new measurement w such that the system (4.90 and 4.91) appears in the canonical form presented in Sect. 2.4. While doing so we highlight also the intuitions that led us to discover this particular change of coordinates.

First, since the term $x_1 + x_3$ occurs frequently in (4.90 and 4.91) a simplifying choice is to assume $z_1 = x_1 + x_3$. With this choice we have $\dot{z}_1 = \dot{x}_1 + \dot{x}_3 = x_2 + u_3$ and therefore it is natural to choose $z_2 = x_2$ to obtain $\dot{z}_1 = z_2 + u_3$, thus matching with the first row of the sought canonical form (2.15).

Now, if we compare the second and third rows of (4.90), with the corresponding rows of the sought canonical form (2.15) we see that: *(i)* in the canonical form (2.15) the state-dependent nonlinearity ϕ appears only in the last row of the dynamics, but, on the other hand *(ii)* in (4.90) the nonlinearity appears already in the second row. Therefore, in order to push this 'undesired' nonlinearity down from the second to the third row we can define $z_3 = \dot{z}_2 = \dot{x}_2 = a_1 c_{x_1} + a_2 c_{x_1+x_3} u_1$. Summarizing, we propose the following change of variables

$$z_1 = x_1 + x_3, \quad z_2 = x_2, \quad z_3 = \dot{x}_2 = a_1 c_{x_1} + a_2 c_{x_1+x_3} u_1, \tag{4.92}$$

that transforms the system (4.90 and 4.91) in the following form

$$\dot{\mathbf{z}} = \underbrace{\begin{bmatrix} 0 & 1 & 0 \\ 0 & 0 & 1 \\ 0 & 0 & 0 \end{bmatrix}}_{\mathbf{A}} \mathbf{z} + \underbrace{\begin{bmatrix} 0 \\ 0 \\ 1 \end{bmatrix}}_{\mathbf{B}} \sigma'(\mathbf{z}, s_{x_1}, u_1, \dot{u}_1, u_3) + \underbrace{\begin{bmatrix} u_3 \\ 0 \\ 0 \end{bmatrix}}_{\boldsymbol{\lambda}(u_3)} \tag{4.93}$$

$$\mathbf{a} = \begin{bmatrix} l c_{z_1} \left(z_2^2 + a_1 s_{x_1} + a_2 s_{z_1} u_1 \right) \\ l s_{z_1} \left(z_2^2 + a_1 s_{x_1} + a_2 s_{z_1} u_1 \right) - a_2 u_1 \end{bmatrix}, \tag{4.94}$$

where the sole state-dependent nonlinearity $\sigma' = a_1 z_2 s_{x_1} + a_2 c_{z_1} \dot{u}_1 - a_2 s_{z_1} (z_2 + u_3) u_1$ is now appearing in the third row, as desired. Notice that we have, on purpose, left the term s_{x_1} untransformed. In the following we show why this choice is convenient instead of directly computing s_{x_1} from (4.92).

To reach the form of (2.15) it remains to extract a measurement of z_1 from the accelerometer reading. From (4.94), defining

$$\eta = \sqrt{a_x^2 + (a_z + a_2 u_1)^2} = \pm l \left(z_2^2 + a_1 s_{x_1} + a_2 s_{z_1} u_1 \right), \tag{4.95}$$

we can obtain a direct measure of z_1 writing

$$w = \operatorname{atan2}\left(\pm a_x / \eta,\ \pm (a_z + a_2 u_1)/\eta \right) = z_1 + k\pi, \tag{4.96}$$

where $k \in \{0, 1\}$. Notice that the transformation is possible only if $\eta \neq 0$. From (4.12), the internal forces expression for the reduced system (4.87) results:

$$f_L = \frac{1}{a_2} x_2^2 + \frac{a_1}{a_2} s_{x_1} + s_{x_1+x_3} u_1. \tag{4.97}$$

Then, from Eqs. (4.97) and (4.95) it results that

$$\eta = \pm \frac{1}{m_R} \left(\frac{1}{a_2} z_2^2 + \frac{a_1}{a_2} s_{x_1} + s_{z_1} u_1 \right) = \pm \frac{f_L}{m_R}, \tag{4.98}$$

thus the transformation (4.96) requires non zero force along the link, $f_L \neq 0$, as in the previous section. Another time, this correspondence highlights, that the condition $f_L \neq 0$ it is not just related to our particular transformation choice but is a structural observability requirement. Indeed, if the force along the link is zero, the aerial vehicle and the link become two independent systems[9] and the onboard inertial sensor is not enough to estimate the entire state. In the design of the observer we need to consider this singularity especially for the cases where the desired link force passes from a tension ($f_L > 0$) to a compression ($f_L < 0$).

The accelerometer is also used to replace s_{x_1} into (4.93) obtaining the sought canonical form(2.15). In particular from (4.95) we can write

$$s_{x_1} = \left(\pm \eta / l - z_2^2 - a_2 s_{z_1} u_1 \right) / a_1. \tag{4.99}$$

With reference to (4.93) we can then write $\sigma' = \sigma(\mathbf{z}, \boldsymbol{\mu})$, i.e., in terms of only $\mathbf{z}$ and known quantities $\boldsymbol{\mu} = [u_1 \ \dot{u}_1 \ u_3 \ \pm \eta]^\top$. Notice that the time derivative of the thrust is needed. This can be computed numerically from u_1 in an approximate way. However, if one of the previous presented dynamic feedback linearizing controllers is used (see Sect. 4.6), $\dot{u}_1$ is an internal state of the controller and so known precisely.

Observe that, the sign to be put in front of η is ambiguous. It is convenient to recast this ambiguity putting always a positive sign and considering two possible values: $\eta_+ = +\eta$ and $\eta_- = -\eta$. Corresponding to these quantities we then get two different dynamic models, the one with $(\sigma(\mathbf{z}, \boldsymbol{\mu}_+), w_+)$ and the one with $(\sigma(\mathbf{z}, \boldsymbol{\mu}_-), w_-)$ corresponding to the use of η_+ and η_-, respectively. At each time instant only one choice for η is correct, i.e., $\eta = f_L / m_R$, to which corresponds the correct measure $w = z_1$ and the correct dynamics. It is not possible, however, to discriminate the correct choice instantaneously from the measurements only. In Sect. 4.8.4 we propose a discriminating solution based on the prediction error.

Although less intuitive, the computation of s_{x_1} into (4.93) exploiting the accelerometer readings, allows to concentrate the ambiguity only on the sign of η obtaining two possible dynamic models. Whereas with the more canonical technique, i.e., inverting the state transformation, we would have four different dynamic models. Indeed

[9] In fact, due to the assumption that the mass and rotational inertia of the link are negligible, the link force represents the only coupling force between the two sub-systems.

from (4.92) we would get $s_{x_1} = \pm\sqrt{1-(z_3 - a_2 c_{z_1} u_1)^2/a_1^2}$ that presents another ambiguity on the sign thus generating four possible combinations of the dynamics and measurement equations.

For the design of the observer let us assume that the correct choice between η_+ and η_- is known. In Sect. 4.8.4 we shall propose a method to gain this knowledge. Under this assumption, the described transformation of the state and the measurements have finally transformed the original system (4.90 and 4.91) in an equivalent one in a canonical form, i.e., $\dot{\mathbf{z}} = \mathbf{A}\mathbf{z} + \mathbf{B}\sigma(\mathbf{z}, \boldsymbol{\mu}) + \boldsymbol{\lambda}(\boldsymbol{\mu})$ and $w = [1\ 0\ 0]\mathbf{z} = \mathbf{C}\mathbf{z}$, for which we can use the following high gain observer [24]

$$\dot{\hat{\mathbf{z}}} = \mathbf{A}\hat{\mathbf{z}} + \mathbf{B}\sigma(\hat{\mathbf{z}}, \boldsymbol{\mu}) + \boldsymbol{\lambda}(\boldsymbol{\mu}) + \mathbf{H}(w - \mathbf{C}\hat{\mathbf{z}}), \tag{4.100}$$

where $\mathbf{H} = \left[\frac{\alpha_1}{\epsilon}\ \frac{\alpha_2}{\epsilon^2}\ \frac{\alpha_3}{\epsilon^3}\right]^\top$, $\epsilon \in \mathbb{R}_{>0}$, and $\alpha_i \in \mathbb{R}_{>0}$ are set such that the roots of $p^3 + \alpha_1 p^2 + \alpha_2 p + \alpha_3$ have negative real part.[10]

4.8.2 Observation of the Original State

From the estimation of $\mathbf{z}$, in order to obtain the estimation of the original state $\mathbf{x}$, we note that the state transformation (4.92) is not directly invertible. One can notice that the only knowledge of $\mathbf{z}$ is not enough to retrieve x_1, indeed from (4.92) one can extract only c_{x_1}. Nevertheless, exploiting also the accelerometer measurements (4.99), we can write

$$\begin{bmatrix} c_{x_1} \\ s_{x_1} \end{bmatrix} = \begin{bmatrix} \dfrac{1}{a_1}(z_3 - a_2 c_{z_1} u_1) \\ \dfrac{1}{a_1}\left(\frac{\eta}{l} - z_2^2 - a_2 s_{z_1} u_1\right) \end{bmatrix} = \boldsymbol{h}(\mathbf{z}, u_1, \eta). \tag{4.101}$$

The state x_1 can then be computed as the phase of the unit vector $\boldsymbol{h}(\mathbf{z}, u_1, \eta)$ denoted by $\angle\boldsymbol{h}(\mathbf{z}, u_1, \eta)$. Thus the estimation of the original state is given by

$$\hat{\mathbf{x}} = \hat{\mathbf{x}}(\hat{\mathbf{z}}, u_1, \eta) = \begin{bmatrix} \angle\boldsymbol{h}(\hat{\mathbf{z}}, u_1, \eta) \\ \hat{z}_2 \\ \hat{z}_1 - \angle\boldsymbol{h}(\hat{\mathbf{z}}, u_1, \eta) \\ u_3 \end{bmatrix}. \tag{4.102}$$

The full observer chain is then depicted in Fig. 4.5.

[10] The difference $(w - C\hat{\boldsymbol{\zeta}})$ stands here for the unique angle $\beta \in (-\pi, \pi]$ such that $\beta + C\hat{\boldsymbol{\zeta}} = w + k2\pi$ for a certain $k \in \mathbb{Z}$.

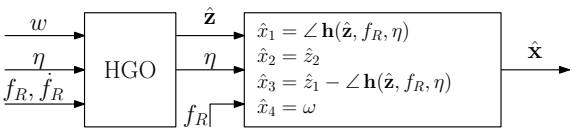

Fig. 4.5 Observer. © 2020 IEEE. Reprinted, with permission, from [12]

4.8.3 Closed-Loop System Stability with State Observation

To prove the stability of the closed loop system when the control action is computed from the estimated state, a similar reasoning to the one in Sect. 4.7 can be done. In particular, for each of the state feedback linearizing controllers, since they are stable out of some singularities (see Table 4.4) there exists $\epsilon^\star > 0$ such that, for every $0 < \epsilon < \epsilon^\star$, the global closed loop system is exponentially convergent for every state except for the zero internal link force and the for the controller singularities. Although the convergence of the observer is almost global, an initialization phase of the estimation can be useful in order to minimize the transient duration, e.g., using the method proposed in [6] for a quasi static initial condition.

Furthermore notice that this observer cannot be directly employed with the static controllers of Table 4.4. Indeed a measure of the derivative of the thrust is needed. Nevertheless one can compute it numerically or applying a dynamic compensator to such controllers. This last option is omitted in this book since it is a trivial extension.

4.8.4 Disambiguation of η and Observability Discussion

As explained before, the transformation of the measurements presents an ambiguity on the sign of η, that can be considered positive, η_+, or negative, η_-. We show in this section how the correct choice can be easily made. Refer to Fig. 4.6 for a graphical representation.

For each of the two possible choices let us implement an HGO equal to (4.100)

$$\dot{\hat{\mathbf{z}}}_+ = \mathbf{A}\hat{\mathbf{z}}_+ + \mathbf{B}\sigma(\hat{\mathbf{z}}_+, \boldsymbol{\mu}_+) + \boldsymbol{\lambda}(\boldsymbol{\mu}_+) + \mathbf{H}(w_+ - \mathbf{C}\hat{\mathbf{z}}_+) \tag{4.103}$$

$$\dot{\hat{\mathbf{z}}}_- = \mathbf{A}\hat{\mathbf{z}}_- + \mathbf{B}\sigma(\hat{\mathbf{z}}_-, \boldsymbol{\mu}_-) + \boldsymbol{\lambda}(\boldsymbol{\mu}_-) + \mathbf{H}(w_- - \mathbf{C}\hat{\mathbf{z}}_-), \tag{4.104}$$

obtaining two different estimations of the state $(\hat{\mathbf{z}}_+, \hat{\mathbf{z}}_-)$, and therefore two different estimations of the original state $(\hat{\mathbf{x}}_+, \hat{\mathbf{x}}_-)$ of which only one is correct. In order to select the correct state we propose a discrimination method based on the comparison of the measurement prediction errors. At the first observer we assign a prediction error $\tilde{e}_+$ smoothed with an exponential discount factor: $\dot{\tilde{e}}_+ = \lambda\left(\left\|\mathbf{a} - \hat{\mathbf{a}}_+\right\| - \tilde{e}_+\right)$, where $\lambda \in \mathbb{R}_{>0}$ sets the discount rate, and $\hat{\mathbf{a}}_+$ is defined as

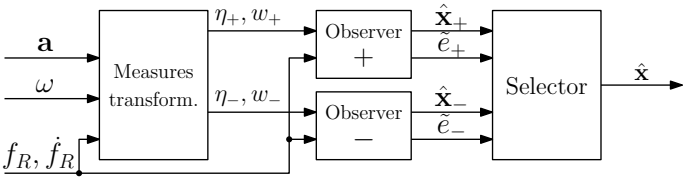

Fig. 4.6 Global observer with disambiguation of η. © 2020 IEEE. Reprinted, with permission, from [12]

$$\hat{\mathbf{a}}_+ = \begin{bmatrix} lc_{\hat{x}_{1+}+\hat{x}_{3+}} \left(\hat{x}_{2+}^2 + a_1 s_{\hat{x}_{1+}} + a_2 s_{\hat{x}_{1+}+\hat{x}_{3+}} u_1\right) \\ ls_{\hat{x}_{1+}+\hat{x}_{3+}} \left(\hat{x}_{2+}^2 + a_1 s_{\hat{x}_{1+}} + a_2 s_{\hat{x}_{1+}+\hat{x}_{3+}} u_1\right) - a_2 u_1 \end{bmatrix}. \tag{4.105}$$

The other prediction error $\tilde{e}_-$ is defined similarly. Then we select the estimation provided by the observer implementation which produces the prediction error closer to zero, i.e., $\hat{\mathbf{x}} = \hat{\mathbf{x}}_+$ if $\tilde{e}_+ \leq \tilde{e}_-$ and $\hat{\mathbf{x}} = \hat{\mathbf{x}}_-$ otherwise.

In Fig. 4.6 we represent the full observer with the discrimination chain. Notice that the disambiguation of the two observers is not done directly using $\hat{\mathbf{z}}$ because is not possible to write the predicted measure $\hat{\mathbf{a}}$ as function of $\hat{\mathbf{z}}$ without introducing another ambiguity. Indeed, as we saw in Sect. 4.8.1, trying to replace $\hat{\mathbf{x}}$ with $\hat{\mathbf{z}}$ into (4.105) inverting the state transformation (4.92), we introduce an ambiguity on the sign of s_{x_1}. Whereas the problem does not hold if we apply this discrimination technique on the original state estimation $(\hat{\mathbf{x}}_+, \hat{\mathbf{x}}_-)$.

Notice that for the motions that implies a constant elevation ($x_2 = 0$), it is not possible to discriminate the correct observer. Indeed, with $x_2 = 0$ and since $w_\pm = z_1 + k\pi$, after a transient the two observers converge to ($\hat{z}_{1\pm} = z_1 + k\pi$, $\hat{z}_{2\pm} = 0$, $\hat{z}_{3\pm} = 0$), and, using (4.102), we obtain ($\hat{x}_{1\pm} = x_1 + k\pi$, $\hat{x}_{2\pm} = 0$, $\hat{x}_{3\pm} = x_3$, $\hat{x}_{4\pm} = x_4$). Under this condition, from Eq. (4.105) it results that the prediction errors of the two observers converge both to zero thus making ineffective the proposed discrimination strategy. Nevertheless, in practice this is not a problem. Indeed, if the controller loop is closed with the wrong observer then the wrong estimation will let the control implement a law that is different from the sole that keeps $x_2 = 0$ causing $x_2 \neq 0$ and thus the predictions errors will become discriminant.

Finally, notice that the ambiguity issue discussed in this section is present only in the initial phases. Whenever the good observer is selected with sufficient certainty, one can switch off the other. For this purpose one can set a confidence threshold on the tracking error of the desired output. If an observer reaches the confidence threshold then this is identified as the correct one and the other one is switched off.

4.9 Discussion on the Proposed Observers

In this book we proposed two observers for the state estimation of a tethered aerial vehicle. One for the general system and one for the reduced one presented in Sect. 4.3.

Table 4.6 List of designed observers with corresponding main features and characteristics

Model	Method	External measurements	Internal measurements	Transformations	Singularities	Degree	Ambiguities
General	HGO	IMU, three encoders	–	Measures	$f_L = 0$	2	No
Reduced	HGO	IMU	$\dot{f}_R$	Measures, state	$f_L = 0$	2	2

The main features and characteristics of such observers are summarized in Table 4.6. Some discussions about the applicability and the robustness of the proposed observers follow.

4.9.1 Applicability

If the link force f_L is zero then some of the measurement transformation shown for both the general and reduced model cannot be determined. In the very special case that the link force has to be constantly equal to zero, the proposed observers are not applicable[11] (while the controller would still work). Nevertheless, the proposed controller Γ^a_{DFL} can guarantee a nonzero link internal force. In the particular case in which the desired link force is passing through zero for a sufficiently short time interval, then the proposed observer can be still used in practice by updating the filter without the correction term in that time instants. For example, for the reduced model we can impose

$$\dot{\hat{\mathbf{z}}} = \mathbf{A}\hat{\mathbf{z}} + \mathbf{B}\sigma(\hat{\mathbf{z}}, \boldsymbol{\mu}) + \boldsymbol{\lambda}(\boldsymbol{\mu}) \quad \text{if } \eta = 0. \tag{4.106}$$

In this way the error dynamics becomes non strictly stable for a short moment but the dynamics returns asymptotically stable as soon as the link force returns to a non-zero value.

4.9.2 Robustness

In order to deal with known drawbacks of the HGO, such as peaking phenomenon and noise sensitivity, many common practical solutions have been presented in the literature, see e.g., [24]. For example, to overcome the peaking phenomenon, it is sufficient to saturate the estimated state on a bounded region that defines the operative regions of the state for the system in exam. In the presence of measurement noise, the use a switched-gain approach can guarantee a quick convergence to the real state during the first phase while reducing the noise effects at steady state.

[11] The static observer in [6] requires a nonzero link force as well to work.

References

1. Oh, S.-R., Pathak, K., Agrawal, S.K., Pota, H.R., Garrett, M.: Approaches for a tether-guided landing of an autonomous helicopter. IEEE Trans. Robot. **22**(3), 536–544 (2006)
2. EC-SAFEMOBIL. EU Coll. Proj. FP7-ICT 288082. http://www.ec-safemobil-project.eu/
3. Sandino, L.A., Bejar, M., Kondak, K., Ollero, A.: Advances in modeling and control of tethered unmanned helicopters to enhance hovering performance. J. Intell. Robot. Syst. **73**(1–4), 3–18 (2014)
4. L. Sandino, D. Santamaria, M. Bejar, A. Viguria, K. Kondak, and A. Ollero. Tether-guided landing of unmanned helicopters without GPS sensors. In: 2014 IEEE International Conference on Robotics and Automation, pp. 3096–3101, Hong Kong, China, May (2014)
5. Sandino, L.A., Bejar, M., Kondak, K., Ollero, A.: A square-root unscented Kalman filter for attitude and relative position estimation of a tethered unmanned helicopter. In: 2015 International Conference on Unmanned Aircraft Systems (ICUAS), pp. 567–576. IEEE (2015)
6. Lupashin, S., D'Andrea, R.: Stabilization of a flying vehicle on a taut tether using inertial sensing. In: 2013 IEEE/RSJ International Conference on Intelligent Robots and Systems, pp. 2432–2438, Tokyo, Japan, Nov (2013)
7. Nicotra, M.M., Naldi, R., Garone, E.: Taut cable control of a tethered UAV. In: 19th IFAC World Congress, pp. 3190–3195, Cape Town, South Africa, Aug (2014)
8. Nicotra, M.M., Naldi, R., Garone, E.: Nonlinear control of a tethered UAV: The taut cable case. Automatica **78**, 174–184 (2017)
9. Siciliano, B., Khatib, O.: Handbook of Robotics. Springer (2008)
10. Tognon, M., Dash, S.S., Franchi, A.: Observer-based control of position and tension for an aerial robot tethered to a moving platform. IEEE Robot. Autom. Lett. **1**(2), 732–737 (2016)
11. Tognon, M., Testa, A., Rossi, E., Franchi, A.: Takeoff and landing on slopes via inclined hovering with a tethered aerial robot. In: 2016 IEEE/RSJ International Conference on Intelligent Robots and Systems, pp. 1702–1707, Daejeon, South Korea, Oct (2016)
12. Tognon, M., Franchi, A.: Dynamics, control, and estimation for aerial robots tethered by cables or bars. IEEE Trans. Robot. **33**(4), 834–845 (2017)
13. Tognon, M., Franchi, A.: Nonlinear observer-based tracking control of link stress and elevation for a tethered aerial robot using inertial-only measurements. In: 2015 IEEE International Conference on Robotics and Automation, pp. 3994–3999, Seattle, WA, May (2015)
14. Tognon, M., Franchi, A.: Position tracking control for an aerial robot passively tethered to an independently moving platform. In: 20th IFAC World Congress, pp. 1069–1074, Toulouse, France, July (2017)
15. Tognon, M., Franchi, A.: Landing and take-off on/from sloped and non-planar surfaces with more than 50 degrees of inclination. In: 9th International Micro Air Vehicles Conference, pp. 97–102 (2017)
16. Tognon, M., Franchi, A.: Control of motion and internal stresses for a chain of two underactuated aerial robots. In: 14th European Control Conference, pp. 1620–1625, Linz, Austria, July (2015)
17. Tognon, M., Franchi, A.: Nonlinear observer for the control of bi-tethered multi aerial robots. In: 2015 IEEE/RSJ International Conference on Intelligent Robots and Systems, pp. 1852–1857, Hamburg, Germany, Sept (2015)
18. Fliess, M., Lévine, J., Martin, P., Rouchon, P.: Flatness and defect of nonlinear systems: introductory theory and examples. Int. J. Control **61**(6), 1327–1361 (1995)
19. Mellinger, D., Kumar, V.: Minimum snap trajectory generation and control for quadrotors. In: 2011 IEEE International Conference on Robotics and Automation, pp. 2520–2525, Shanghai, China, May (2011)
20. Faessler, M., Franchi, A., Scaramuzza, D.: Differential flatness of quadrotor dynamics subject to rotor drag for accurate tracking of high-speed trajectories. IEEE Robot. Autom. Lett. **3**(2), 620–626 (2018)
21. Bullo, F., Lewis, A.D.: Control of Mechanical Systems: Modeling, Analysis, and Design for Simple Mechanical Control Systems, vol. 49. Springer Science Geometric & Business Media (2004)

22. Murray, R.M., Rathinam, M., Sluis, W.: Differential flatness of mechanical control systems: a catalog of prototype systems. In: ASME International Mechanical Engineering Congress and Exposition, San Francisco, CA, Nov (1995)
23. Murray, R.M., Li, Z., Sastry, S.S.: A Mathematical Introduction to Robotic Manipulation. CRC (1994)
24. Khalil, H.K.: Nonlinear Systems, 3rd edn. Prentice Hall (2001)
25. Gioioso, G., Ryll, M., Prattichizzo, D., Bülthoff, H.H., Franchi, A.: Turning a near-hovering controlled quadrotor into a 3D force effector. In: 2014 IEEE International Conference on Robotics and Automation, pp. 6278–6284, Hong Kong, China, May (2014)
26. Mahony, R., Hamel, T., Pflimlin, J.-M.: Nonlinear complementary filters on the special orthogonal group. IEEE Trans. Autom. Control **53**(5), 1203–1218 (2008)